SUPPORTING INFORMATION

Conductometric Gradient Ion Exclusion Chromatography for Volatile Fatty Acids

C. Phillip Shelor, Purnendu K. Dasgupta,* Hongzhu Liao

Department of Chemistry and Biochemistry, University of Texas at Arlington, Arlington, Texas 76019-0065, United States

* E-mail: Dasgupta@uta.edu. Fax: 817-272-3808

Fabrication of FAVE devices.

Eight different designs were tested for the ability to extract VFA's. Table 1 lists the different combinations used. Specifically we wished to investigate length, jacket diameter, the vapor permeable membrane tubing (VPMT) size, coiling, use of polysiloxane vs. Nafion coating, and the effect of adding a nylon filament. FAVE 1 and FAVE 2 are similar to those in a previous study[1] and do not contain the acid penetration section.

Vapor Permeable Membrane Tubing (VPMT). Samples of two sizes of polysiloxane coated porous polypropylene (PPP) tubing were provided by ThermoFisher/Dionex; these tubes are used for the removal of CO_2 from suppressed carbonate eluents in SCICE. The polysiloxane is plasma polymerized on the PPP. The two sizes were 209 µm and 300 µm in inner diameters and 30 µm in wall thickness. An untreated PPP tube of 300 µm inner diameter and 30 µm wall was coated with a colloidal Nafion® solution (5% w/w solution in lower alcohols and 10% H_2O). Nafion® is a sulfonated fluoropolymer. Coating was first accomplished by first inserting a nylon fishing line (~0.2 mm) through the length of the tubing. The fishing line keeps the tubing from collapsing and the bore being filled by the polymer. The PPP tube was then drawn through the Nafion® solution, hung vertically and allowed to air dry. The process was repeated twice. On the last treatment, the fishing line was removed before the tube was dry. The alcoholic Nafion® solution wets the tube allowing the Nafion to enter the PPP pores essentially making the tubing nonporous.

Filament insertion into the VPMT lumen. A filament can be inserted in the VPMT lumen with an intent to improve mass transfer to the membrane wall. This was accomplished before tightening the fitting at the outlet of the device. A nylon fishing line (~210 μm in diameter), the same length as the jacket, was inserted into the VPMT outlet. The FAVE was connected to a pump to deliver 100 μL/min of water. The pumping helps lubricate the insertion of the nylon filament and keeps the tube expanded. While holding the FAVE device taut, the filament is fed through. When all of the precut filament length is inserted, another filament is used to finish pushing it in the rest of the way. The pump is stopped and the outlet fitting is tightened to prevent the filament from flowing back out.

Construction of the FAVE. The fabrication of FAVE device no 6 is described below. Similar steps are followed for the others. The terminus of a 1.2 m long VPMT was sleeved with a 0.4/1.6 mm i.d./o.d., 4 cm long polytetrafluoroethylene (PTFE) tube and connected to the column outlet. The PTFE tube swages to form a seal around the VPMT so that the column effluent flows into the latter. The other end of the PTFE tube is connected to one of the straight arms of a $^{1}/_{16}$" poly(ether ether ketone) (PEEK) tee where the PTFE sleeve again forms a seal around the VPM. A much larger bore (2.4 mm i.d.) 5 cm long PTFE tube, then forms the acid introduction jacket between the first and a second PEEK tee. The far side of the latter also uses a 4 cm length of 0.4 mm bore PTFE tube to seal around the VPM and isolate the 2 jacket sections, and then connects to a third tee. The first two PEEK tees have 1.25 mm through holes while the latter two tees for have 0.5 mm through holes. The VPM is then fed through the PTFE extractor tube (i.d./o.d. 0.38/1.6 mm, 80 cm long) by first inserting and bonding (epoxy

adhesive) a 0.25 mm dia. nylon fishing line 1-2 cm into the tip of the VPMT. The fishing line is fed through the PTFE tube, a fourth tee, and into a final short length of PTFE tubing that seals the extractor section. The nylon line is then pulled through. The line, and most of the attached excess VPMT removed. Nuts on the extraction tube must be gradually tightened until liquid leakage at these junctions no longer occur but also ensuring that the PTFE tube does not seal around the VPM. Excess VPM was cut off from the outlet before installing the FAVE in the system. Finally, the extraction section is coiled around a 1/16” rod and affixed in place (Figure S2).

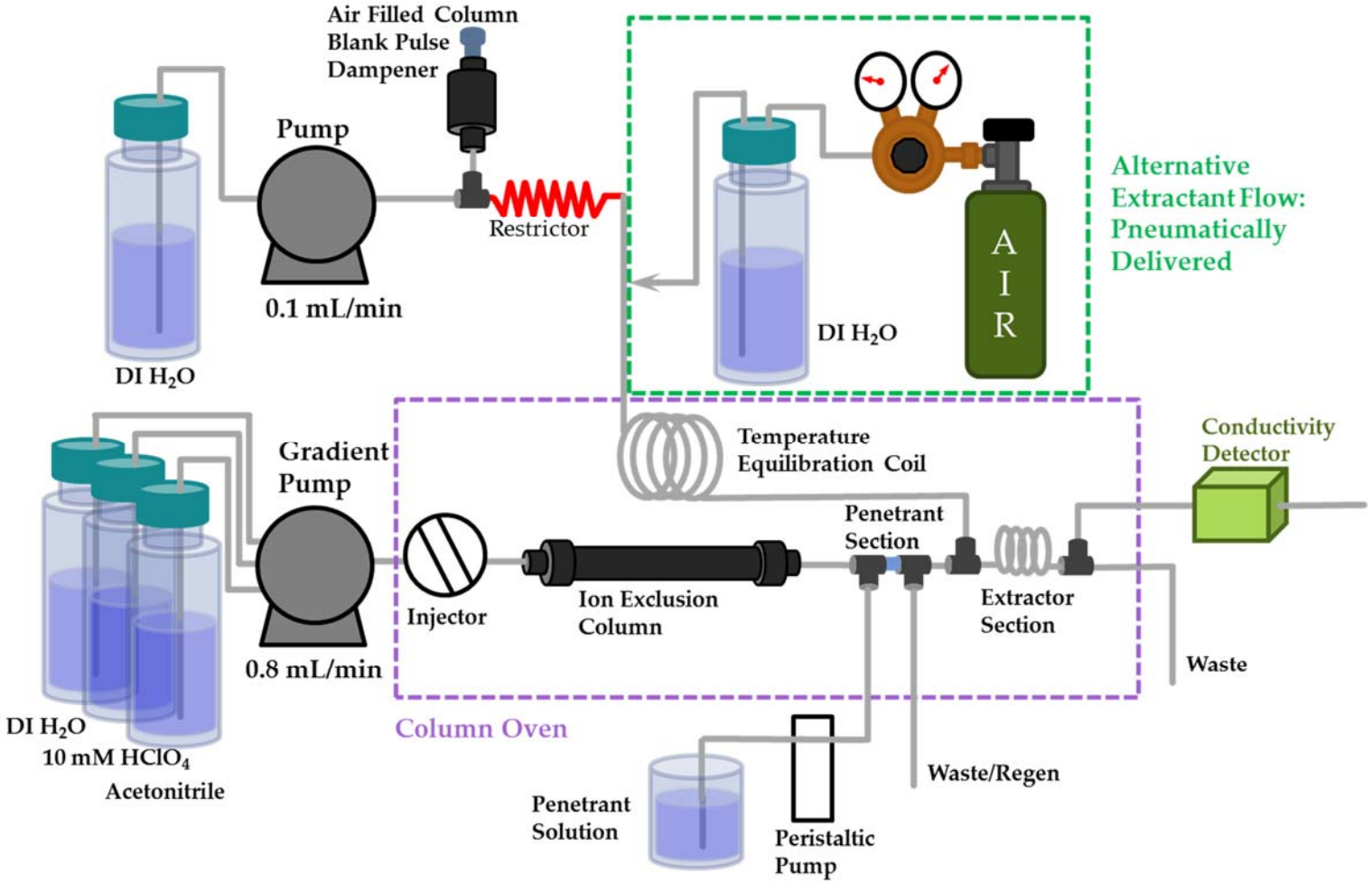

Figure S1: The analytical setup. The column, injector, and extractor are all in the column oven maintained at 60 °C. Also inside the oven is an equilibration coil through which the extractant flows before entering the FAVE. A peristaltic pump is used to recirculate penetrant acid through the FAVE device. Conductivity detection is performed outside the column oven in a 35 °C thermostated cell. The extractant may be delivered pneumatically or by either another HPLC pump (Dionex ICS-2000). To reduce pulsation noise from this pump, a pulse dampener, consisting of an air-filled column blank (9.2 mm i.d., 26 mm long) with one end plugged and oriented up and a restrictor that produced ~300 psi @ 0.1 mL/min was used; both were connected to a tee as shown. Pneumatic pumping of the extractant was used in some experiments as indicated.

Instrumental Arrangement. Chromatography was conducted with a GP-40 gradient pump (0.8 mL/min, except as stated), an ICE-AS1 column (9x250 mm), a LC30 column oven, a CD25 conductivity detector (all from www.dionex.com), a 6-port injector with 20-µL loop (except as stated, www.vici.com). Absorbance detection utilized an Agilent 1290 Diode Array Detector. The column, injector, pump gradient mixer, and the FAVE were all placed inside the column oven (60 °C except as stated). All chromatography and data acquisition was performed using Dionex PeakNet 6 software. The FAVE was connected directly after the column. A peristaltic pump with Viton pump tubing (www.rainin.com) circulated 20% HNO_3 through the acid introduction jacket at ~<0.35 mL/min. The amount of acid lost by penetration is so small, 100 mL can be recycled for at least a week. 18.2 MΩ.cm deionized H_2O (https://ariesfilterworks.com/) was used as extractant and delivered pneumatically or by a pump (Figure S1). The extractant was delivered through a PEEK coil (0.03" i.d. 3 m long) kept in the column oven to allow thermal equilibration before entering the FAVE. Co-current flow was used in the FAVE, this reduces dispersion and peak resolution relative to countercurrent flow.[1] The extractor tee outlet was connected to the conductivity cell by 125 µm i.d. PEEK tubing.

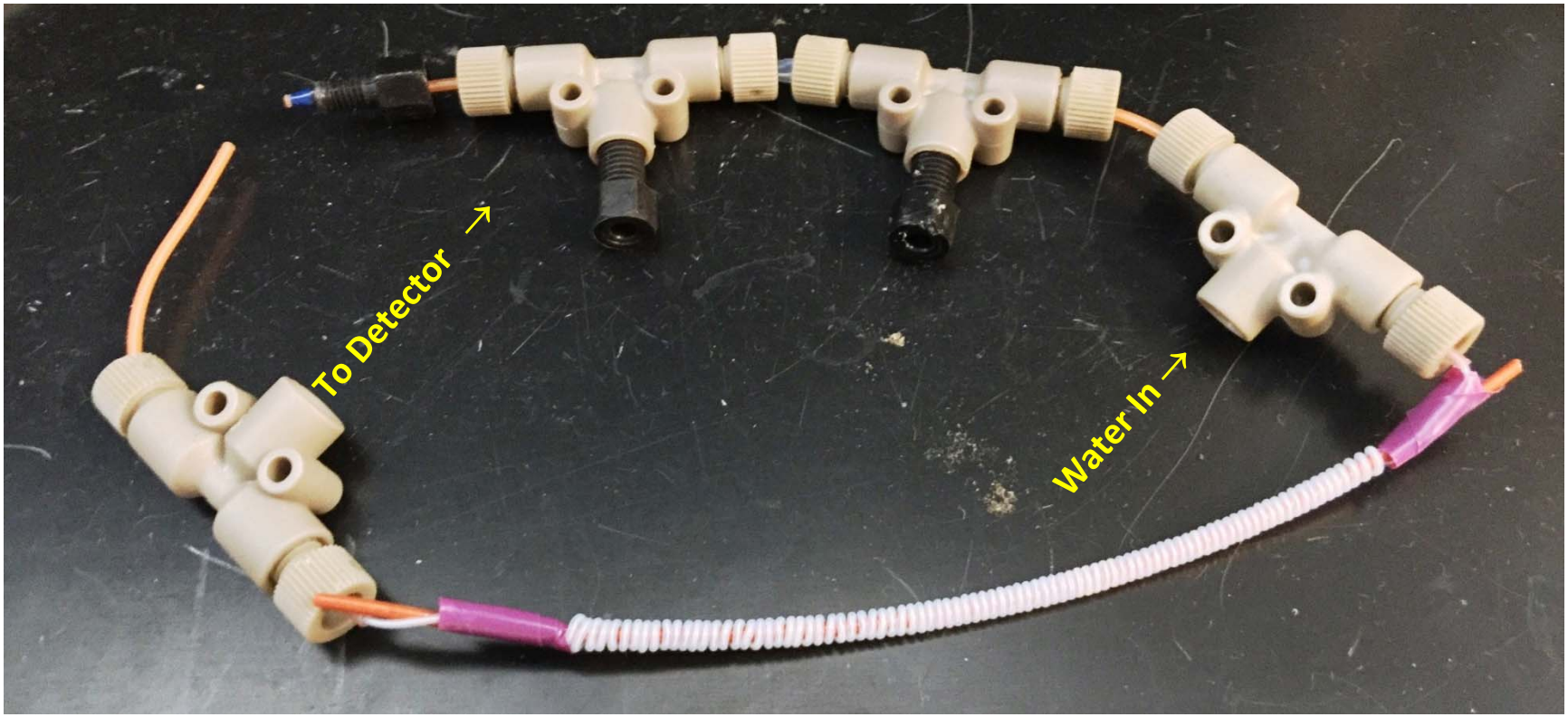

Figure S2. Photograph of the Type 6 FAVE device. The blue-ferruled tube is the inlet for the column effluent.

Theoretical considerations on mass transfer. The rate of mass transfer (*dm/dt*) is dependent on the transmembrane partial pressure difference (p_{lum}-p_{ext}), membrane thickness (δ), membrane area (A) and the permeability coefficient *P*

$$\frac{dm}{dt} = \frac{AP(p_{lum} - p_{ext})}{\delta} \quad ...(S1)$$

The partial pressure *p* and the solution concentration is related by the Henry's law constant (K_H, M/atm). For weak acids, only the undissociated form HX is volatile. For the total concentration in the lumen ($C_{T,lum}$), the partial pressure in the lumen (p_{lum}) will be given by:

$$p_{lum} = \alpha_0 C_{T,lum}/K_H \quad ...(S2)$$

Where α_0 is the fraction of the total concentration that exists as HX. In the present system, most experiments are conducted with a lumenal pH of 2, so for analyte acids with $pK_a \gtrsim 4$, $\alpha_{0,ext}$ can be approximated as unity. On the receptor side, with pure water, the pH is determined by the permeated analyte. Neglecting contributions from autoionization of water and any dissolved CO_2, p_{ext} will be given by:

$$p_{ext} = (C_{T,ext} - \frac{-K_a + \sqrt{{K_a}^2 + 4C_{T,ext}K_a}}{2})/K_H \quad ...(S3)$$

S3 and S2 can be put back into Eq S1. However considerable simplification is possible. When the extent of analyte transfer is small, p_{ext} can be considered negligible with respect to p_{lum} and the transport rate will be linearly related to the analyte concentration as indicated in eq 1 in the main text.

The linear relationship will not hold, however, if a large amount of analyte is transferred such that p_{ext} cannot be neglected with respect to p_{lum}. If a large amount of analyte is transferred, mass transport to the membrane may also become a rate limiting process, which has not been presently considered.

FAVE Device Optimization

All FAVEs were compared using the same separation conditions. Table 1 provides the important dimensions and features of the 8 different devices tested. The eluent was 1 mM $HClO_4$ and the sample was a mixture of formic (60 mg/L), acetic (60 mg/L), propionic (80 mg/L), butanoic (80 mg/L), and pentanoic acids (100 mg/L). No acid penetrant was used for the comparison of the various designs; the eluent provided enough ionization suppression to ensure volatility of a measurable amount of the VFA's and allow a fair comparison to devices 1 and 2 which do not have a penetrant section.

The dimensions of the VPMT determine the extent of analyte transfer to the extractant channel. The area of the membrane increases linearly with the diameter and length. thus increasing overall analyte transfer. Although an increase in the membrane area through an increase in the diameter will result in greater dispersion than through an increase in length, longer length extractors are more difficult to construct. Additionally, the pressure tolerance (200 psi) of these 30 μm-thick-wall membrane must also be considered for both the effluent and extractant flow for the given application. According to the Hagen-Poiseuille equation, the pressure drop across a tube of length L and diameter d will be proportional to L/d^4 at a given solution flow rate and viscosity. Even small increases in diameter may allow much longer lengths of tubing to be used.

Designs #1 and #2 have 6 cm and 25 cm length respectively and were used previously for the extraction of H_2S and HCN following SCIC. The 25 cm extractor provided ~58% and 33% extraction efficiencies for H_2S and HCN, respectively.[1] Peak areas are shown in Figure S3 for different FAVE designs and different analytes. Assuming peak areas to be a measure of the amount of analyte transferred. In going from the 6 cm to the 25 cm tube (a ~4.2x increase in membrane area), peak areas increased on average 4.3 ± 0.6 times. The linear relationship between length and peak area suggest only a small amount is being transferred; extraction efficiency (EE) must be quite small. This is not surprising given that the K_H for VFA's are 2 and 4 orders of magnitude greater than those of HCN and H_2S. ICE peak volumes are substantially larger than in IC, both due to lower efficiency and much larger column bore. We opted to use both larger diameter and longer FAVEs in FAVE 3 through FAVE 6. A newer lot of the siloxane VPMT was used in FAVE 5 and FAVE 6. Devices 3-5 also had a nylon fishing line inserted into the lumen of the VPMT in an attempt to improve mass transfer to the wall. FAVE 3 and FAVE 4 showed on average 5.6 ± 0.3 and 5.5±0.7 times increased average EE for the 5 ions compared to those for device 2. The length was increased 3.2 times while the total membrane area was increased 4.6 times for devices 3 and 4 compared to device 2. Similarly FAVE 5 and FAVE 6, which had the same membrane area as FAVE 3 and FAVE 4, showed an increase in peak area of 3.6 ± 0.2 and 3.6 ± 0.3 times, respectively. The coating thickness of the polysiloxane VPMTs or the base membrane porosity must differ significantly from one batch to another based on the more than 50% increase in extraction efficiency in FAVE 3 and FAVE 4 compared to FAVE 5 and FAVE 6. FAVE 5 and FAVE 6 differ slightly in extractant

jacket diameter, and inclusion of a lumenal filament. Because jacket diameter plays no role in extraction as evidenced by devices comparing FAVE 3 and FAVE 4, one can also conclude that the nylon filament does not increase the EE in the present situation. This confirms the conclusion that the devices are not limited by transport to the wall. As the thickness is already very small, a further increase in transmembrane transport will need to be brought about by an increase in the membrane surface area. This may be more easily accomplished by an increase in the VPMT radius rather than increasing the length of the device. With an increased bore, filament insertion may yet prove useful to keep chromatographic dispersion manageable for a larger i.d. tube.

Extraction Jacket dimension was also investigated. As already indicated this had no effect on the EE for a given membrane batch. However, chromatographic efficiency (Figure S4) greatly benefited from smaller diameter jacket tubing as used in extractors FAVE 6 to FAVE 8. For the siloxane-coated VPMTs, this increase in efficiency led to the best peak heights for FAVE 6 (Figure S5), even though FAVE 3 used a more permeable membrane from a different batch and the overall transport was 50%. While dispersion is undoubtedly increased in the larger jacket, peak tailing, as measured by asymmetry (Figure S6) did not significantly increase. FAVE 3 has as good or better symmetry of peaks than FAVE 6 despite the larger annular gap. However, this is likely because the asymmetry in FAVE 3 counteracted the original asymmetry in the peaks in the column effluent (*vide infra*). The intermediate jacket diameter (FAVE 5) had the worst asymmetry. The asymmetries arise, as described in the main text from the lack of isokinetic flow in the donor and acceptor streams. FAVE 3 for example has the smallest VPMT lumen volume because of the nylon filament, and the largest jacket volume.

Pressure drop or dilution of extracted material considerations make it essentially impossible for the extractant flow velocity to ever match the lumenal velocity. What is interesting here is that depending on the extractant/lumenal velocity ratio, either fronting or tailing can be induced. The peaks in the column effluent are always tailing (see Figure S20 on peak asymmetries which range from 1.18-1.5 for C5 to C1) as observed by a UV detector), fronting in the FAVE extractor can hen restore the asymmetry while tailing will make it worse still.

Comparison of coating materials. Aside from the polysiloxane we also studied a Nafion-coated VPMT made in house. The EE for FAVE 8 was on average 55 ± 6% of that of the comparable siloxane coated VPMT (FAVE 6). However, the film thickness was quite different. Microscopic observation indicated the outer Nafion layer is 3-5 μm thick. In addition if the Nafion actually filled the pores, which is likely, then the effective layer was over 30 μm thick. It is interesting to note that the relative transfer was not uniform across the VFAs. Formate showed the greatest decrease in EE going from the siloxane to Nafion coated tubes (-54% relative), while acetate showed the least (-38% relative). In going from acetate to pentanoate, the transfer decreased monotonically with carbon number, being only 62%, 59%, 54%, and 52% of that for the siloxane coated tube for C2-C4, respectively. This is not surprising since Nafion is highly polar and would be expected to have greater selectivity for polar compounds. Transfer through Nafion must take place as the neutral acid; acetic acid may provide the optimum combination of polar character and pK_a. We did carry out some preliminary experiments using tubes made purely of Nafion and generally observed overall much greater analyte transport despite the greater wall thickness, suggesting the pores in the

PPP must be filled with Nafion in the previous experiment: the transport is greater with tubes made of Nafion because the entire surface, not just the pores, is available for transport. High surface area thin film planar devices as used in current generations of electrodialytic analyte suppression,[2] could provide a more practical alternative of building FAVE devices that can use thin ion exchanger and other elastomeric membranes in a screen-supported manner. Even when the intent is not to do so, current generation of IC suppressors was shown to remove up to 12 and 25% of HCN and H_2S respectively through the cation exchange membranes.[1] Smaller but measurable loss of acetic acid occurs through suppressor membrane at high acetate concentrations.

The effect of coiling was studied extensively by the senior author in developing filament filled tubular suppressors for IC.[3] Coiling the tube improved mass transfer to the wall (as is known from many past studies) resulting in more efficient exchange. Additionally, for helical flow, the parabolic front observed in laminar flow through a tube is flattened some, thus reducing longitudinal dispersion. A similar effect was seen on a comparison of FAVE 3 and FAVE 4. While no consistent increase in peak area was seen, the peak height and efficiency both increased in going from the uncoiled to the coiled device. Peak height increased 12.9 ± 2.2% averaged over C1-C5. Dispersion is improved though upon being coiled as evidenced by the smaller widths and increased height and efficiency. Without coiling, C1 and C2 resolution was poorer and accurate peak widths and asymmetry could not be obtained for the uncoiled device. Similarly, the Nafion coated VPMT was tested in an uncoiled (FAVE 7) and coiled (FAVE 8) configuration. In this case performance was nearly identical; both devices have much

smaller extractant jacket diameters compared to FAVE 3 and 4. What little dispersion occurs in FAVE 7 or 8 could not be further improved upon coiling. However, since it is not detrimental to the extraction process and can only help reduce dispersion, coiling is to be preferred especially when lower extractant flow rates or larger jackets are used.

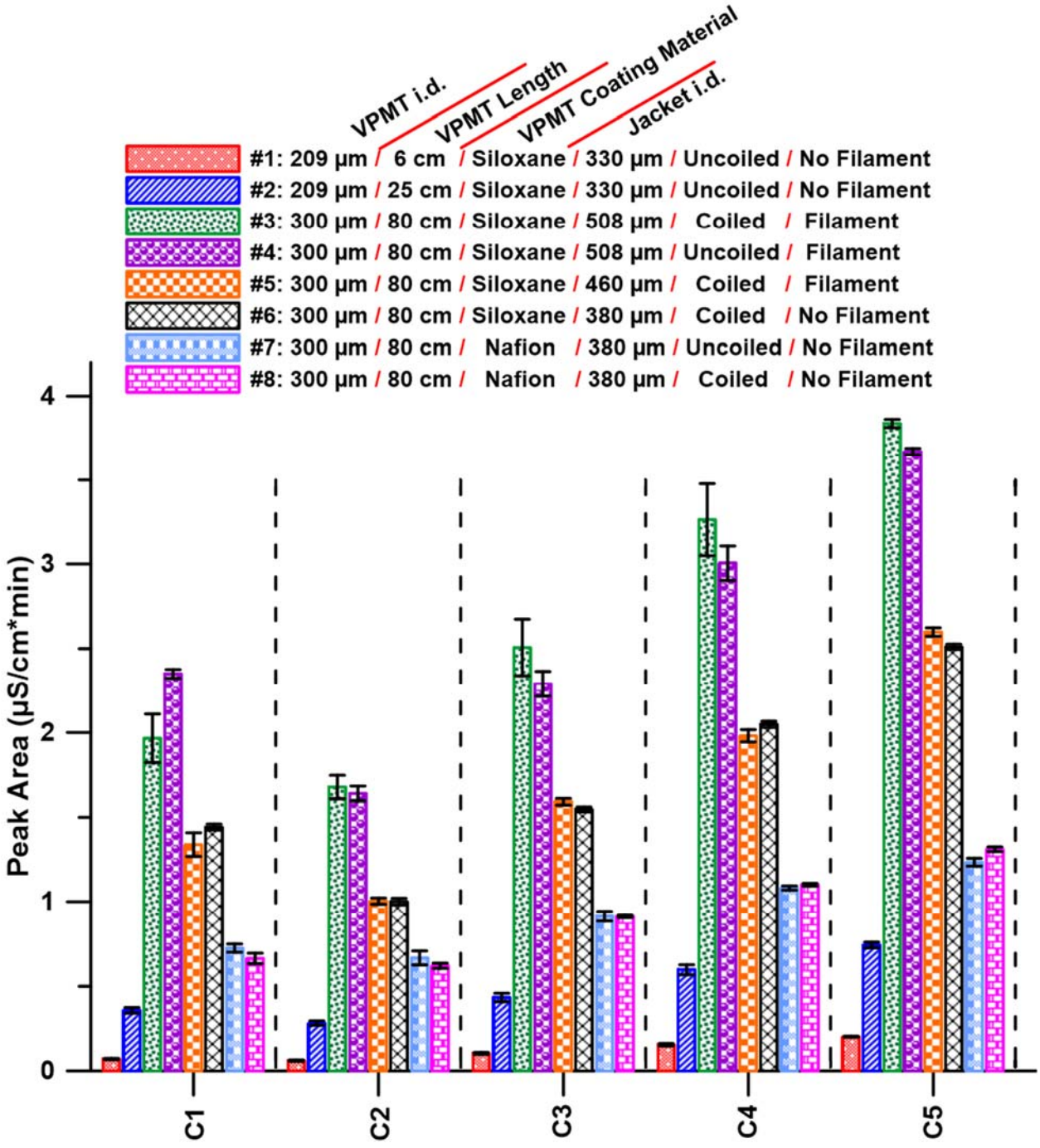

Figure S3. The peak area of the different FAVE designs are shown for the five acids: formic (60 mg/L), acetic, (60 mg/L), propionic (80 mg/L), butanoic (80 mg/L), pentanoic (100 mg/L). 20 µL injection. The top inset has the description of the 8 different extractors.

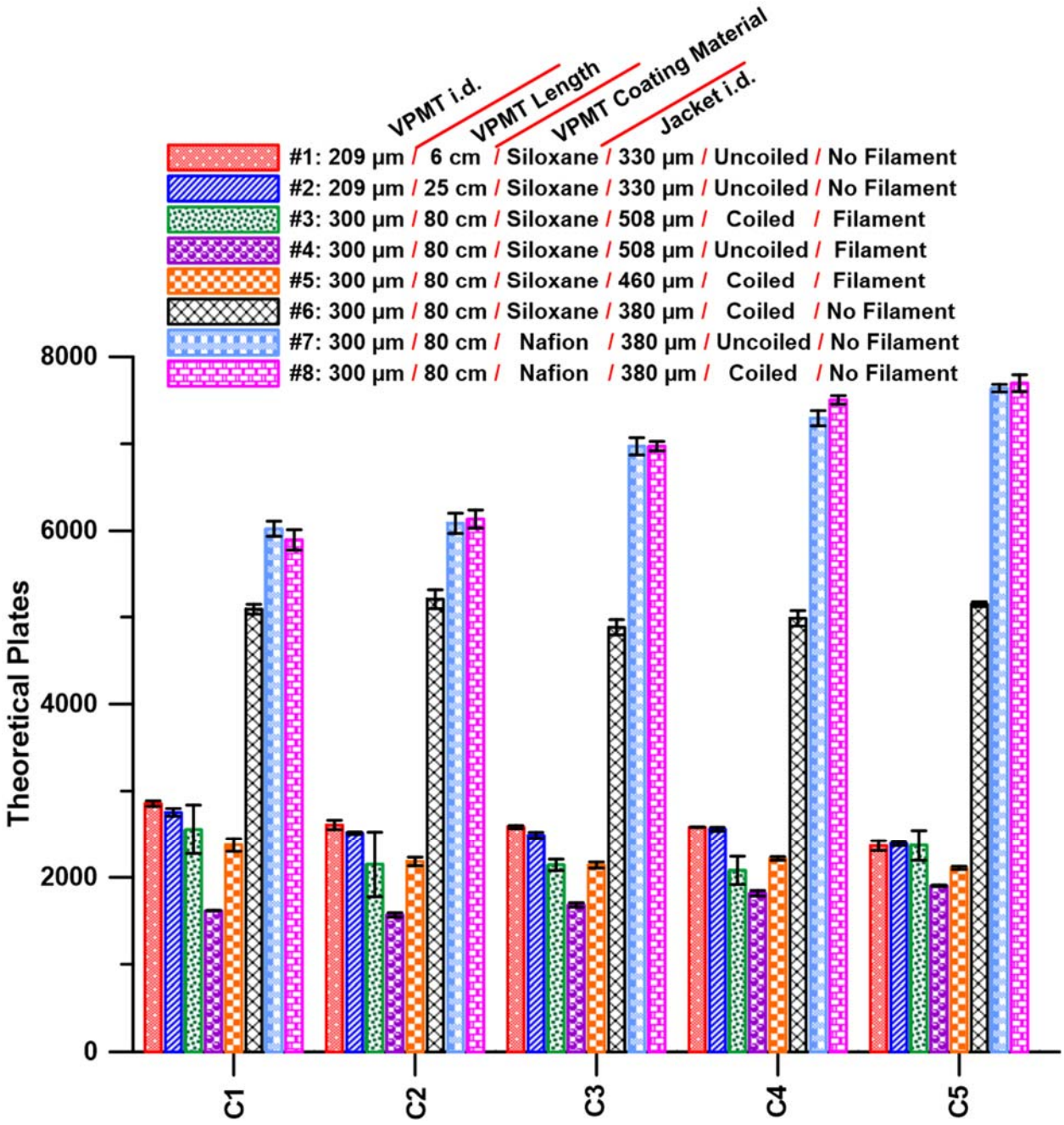

Figure S4. The peak efficiencies of the different FAVE designs are shown for the five acids. See Figure S3 for other conditions

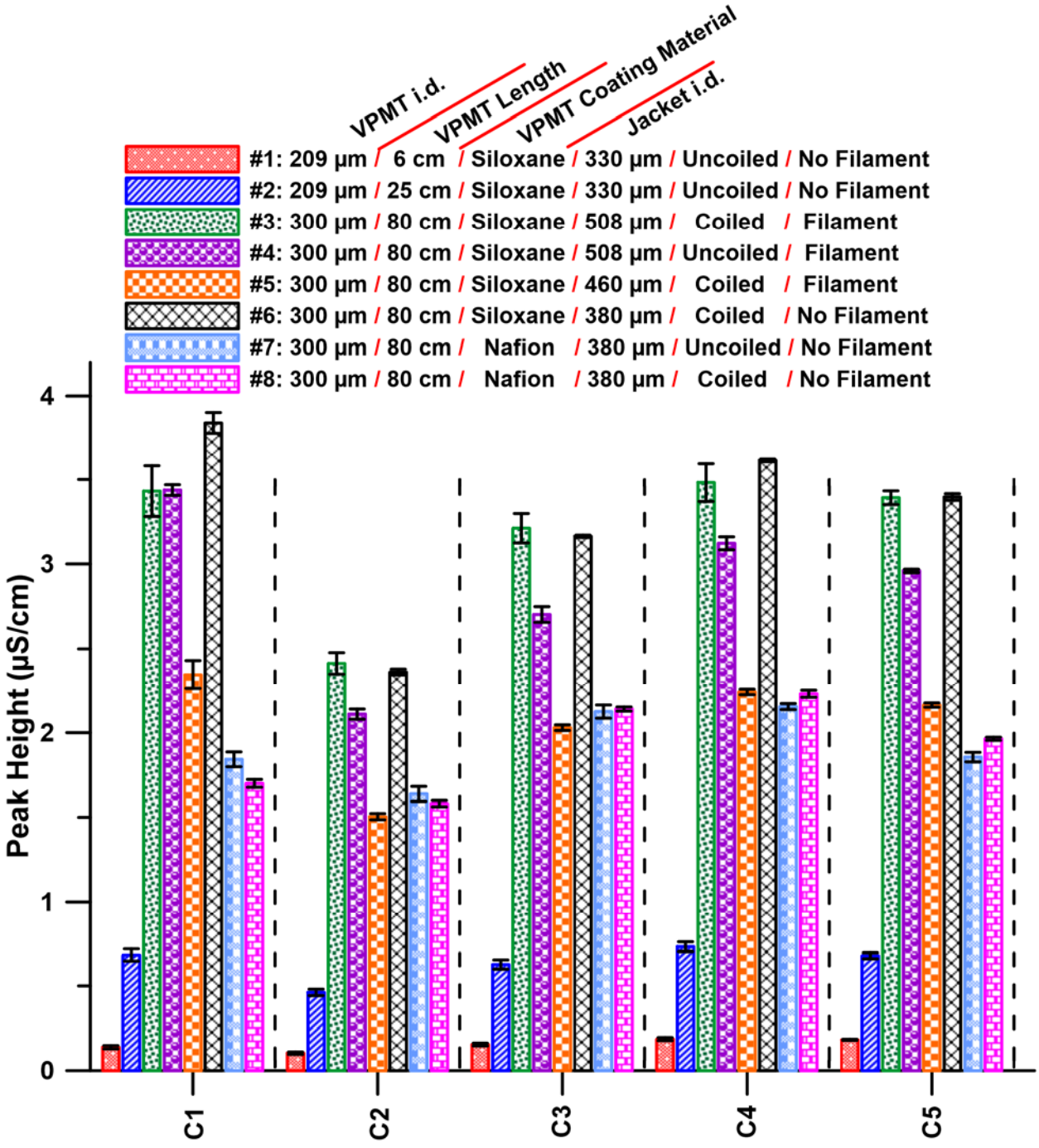

Figure S5. The peak height of the different FAVE designs are shown for the five acids. See Figure S3 for other conditions.

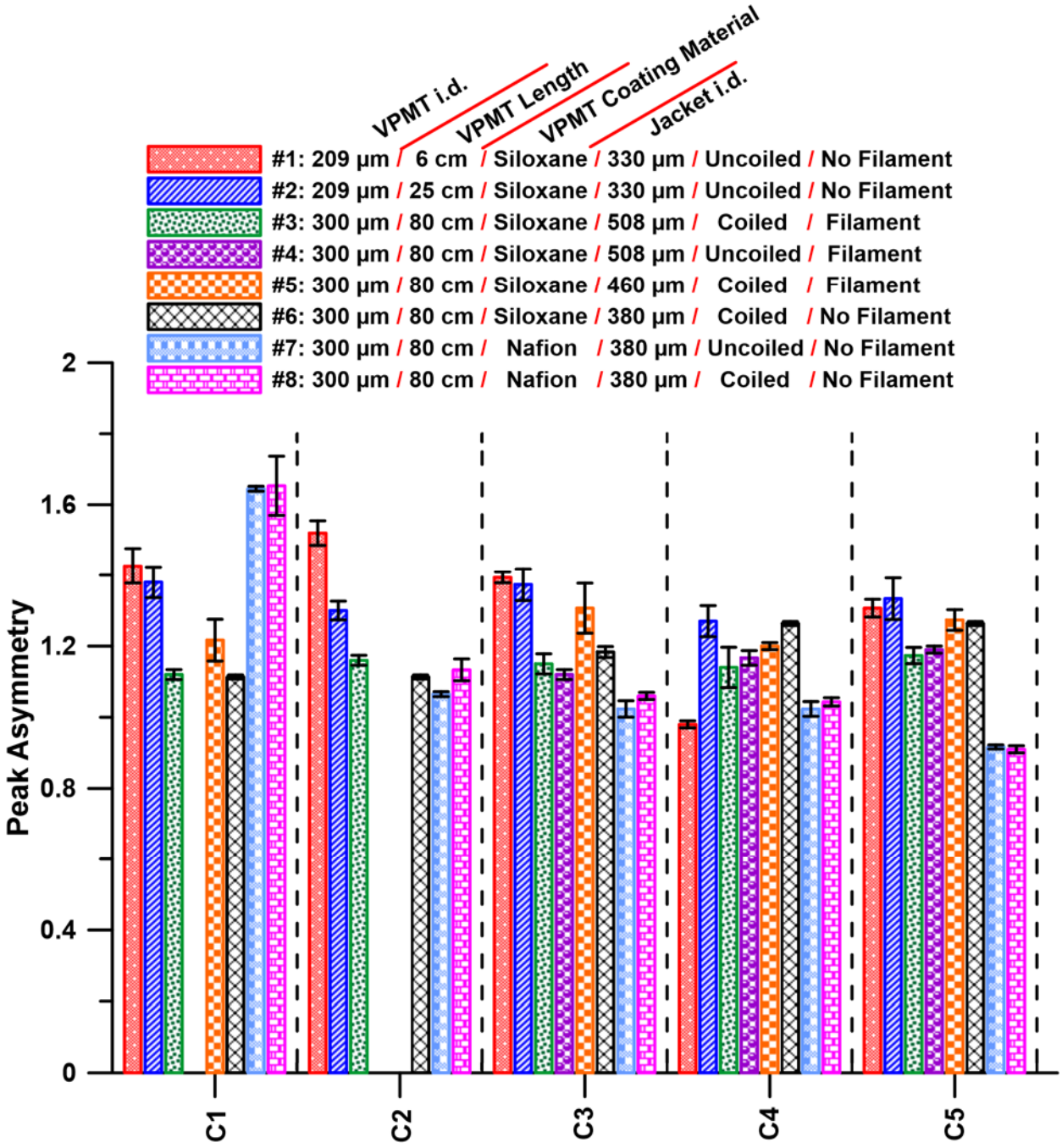

Figure S6. The peak asymmetry of the different FAVE designs are shown for the five acids. Gaps for formate and acetate are seen because these peaks were not entirely resolved for FAVE 4 or 5. See Figure S3 for other conditions.

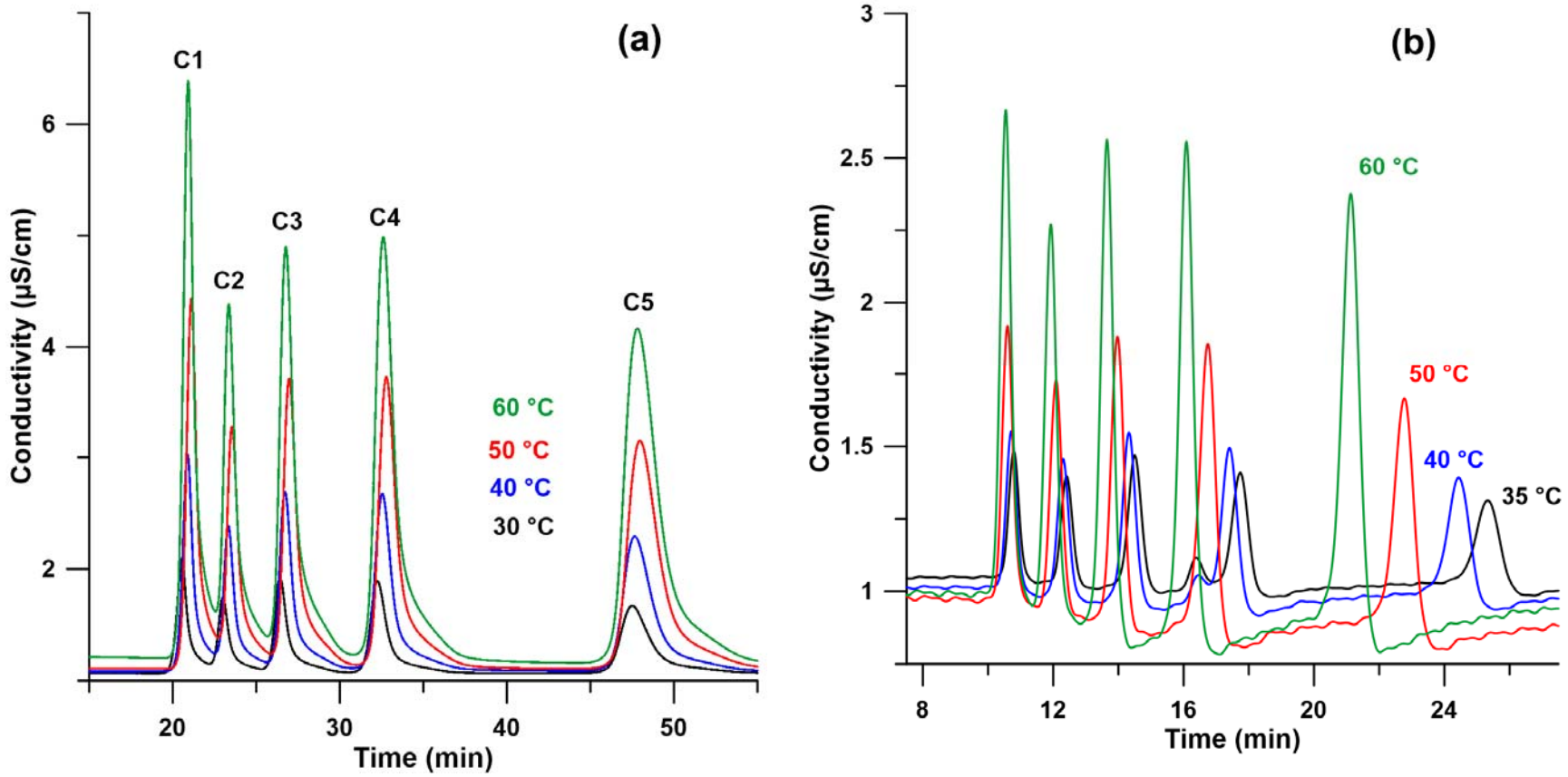

Figure S7. (a) Chromatograms of 5 organic acids at various temperatures. The eluent flow rate is 0.5 mL/min. The extractant flow rate is 0.1 mL/min. Same sample and injection as in Figure S3. The extractor here was a version of design 3 (Table 1), the column was located outside the oven at room temperature ~22 °C. **(b)** Same sample as in (a), flow rate 0.8 mL/min, column located in oven, Nafion coated membrane, FAVE design #8.

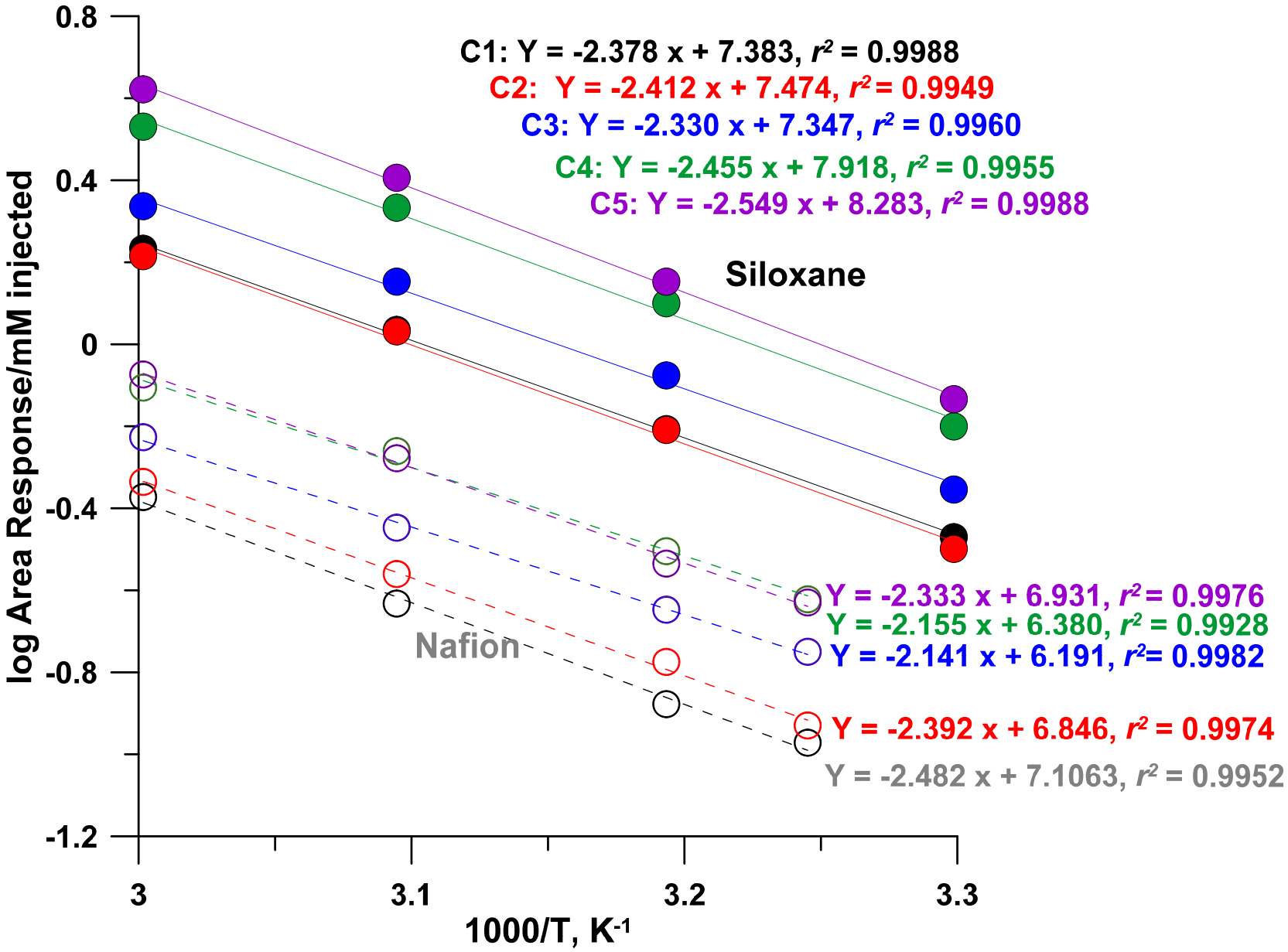

Fig. S8. Arrhenius plots (30-60 °C for siloxane, 35-60 °C for Nafion) for temperature dependence of the FAVE response, conductivity detector.

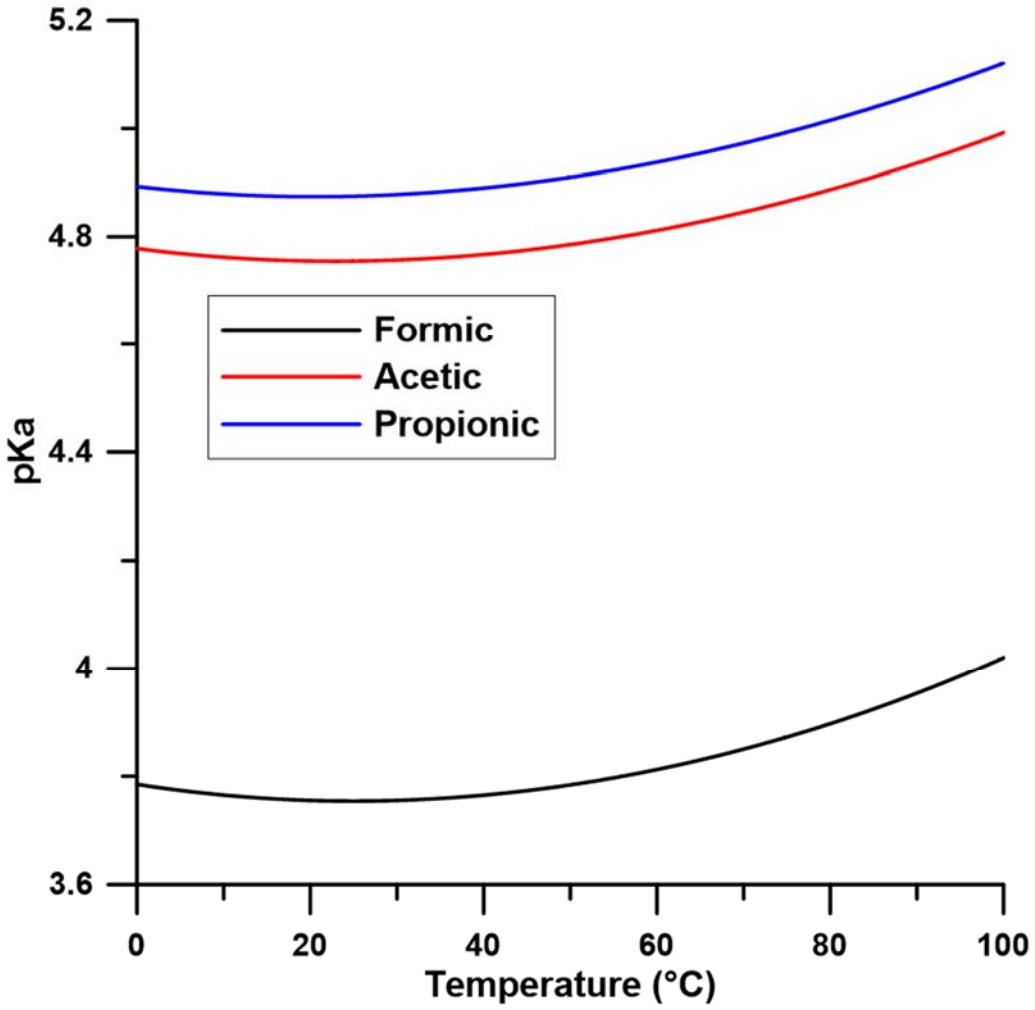

Figure S9. Temperature dependence of pK_a's of C1-C3 acids. Calculated based on equations given in [4].

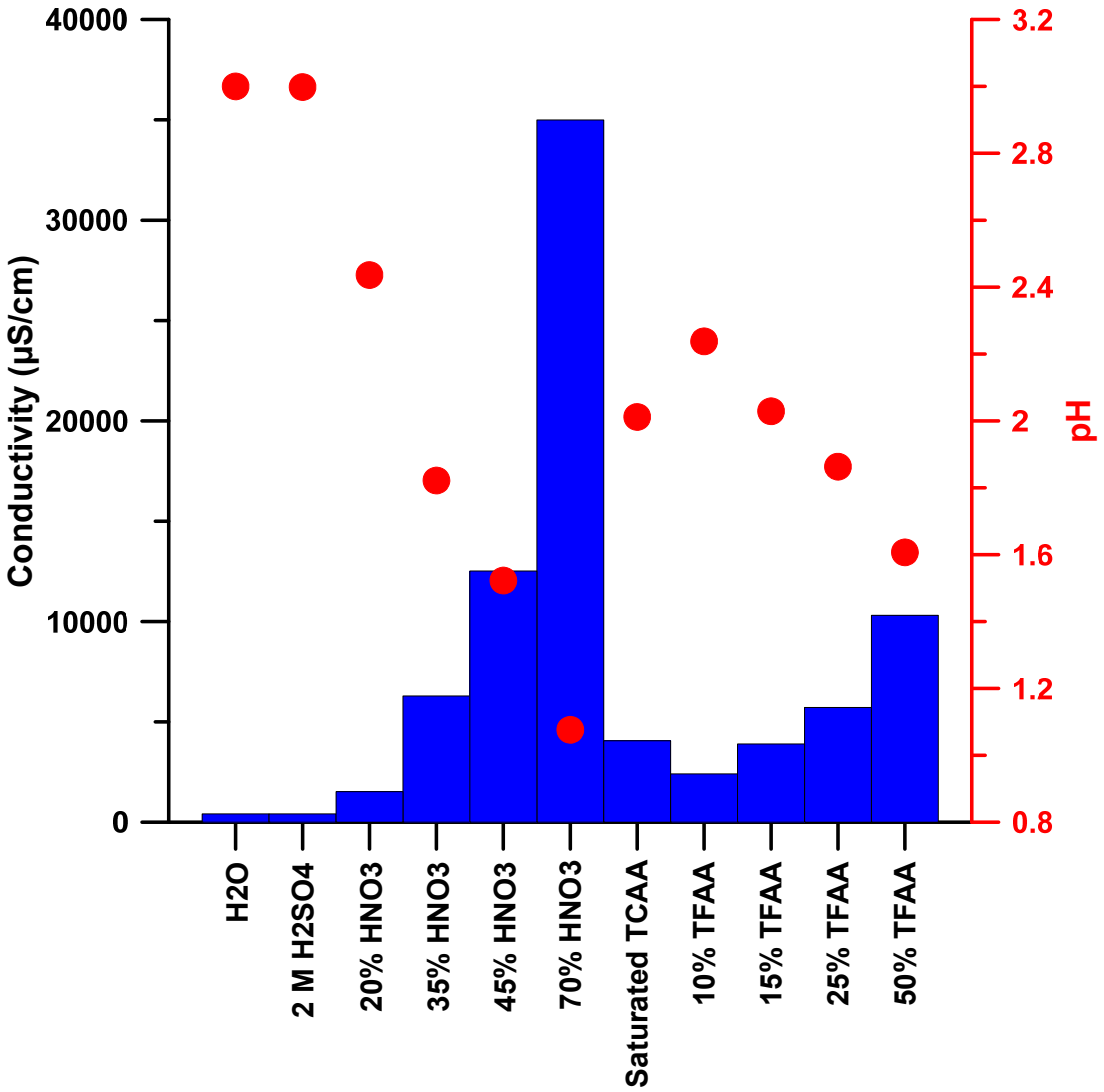

Figure S10. The blue bar chart shows the solution conductivity for the eluent using various penetrants. The eluent contained 1 mM $HClO_4$. Tested penetrant solutions are indicated on the *x*-axis. The corresponding pH is shown as red dots. For reference, formate (pK_a = 3.75) will be 1.7, 15 and 64% dissociated, respectively at pH 2, 3, and 4. The conductance cell used was 2 stainless steel HPLC tubes (250 µm i.d.) connected by a PEEK union. A Dionex CDM-1 was connected to the tubes, calibrated with KCl solutions and used to monitor the conductance. Readings were taken when the conductivity reached stable values. pH was calculated based on solution conductivity.

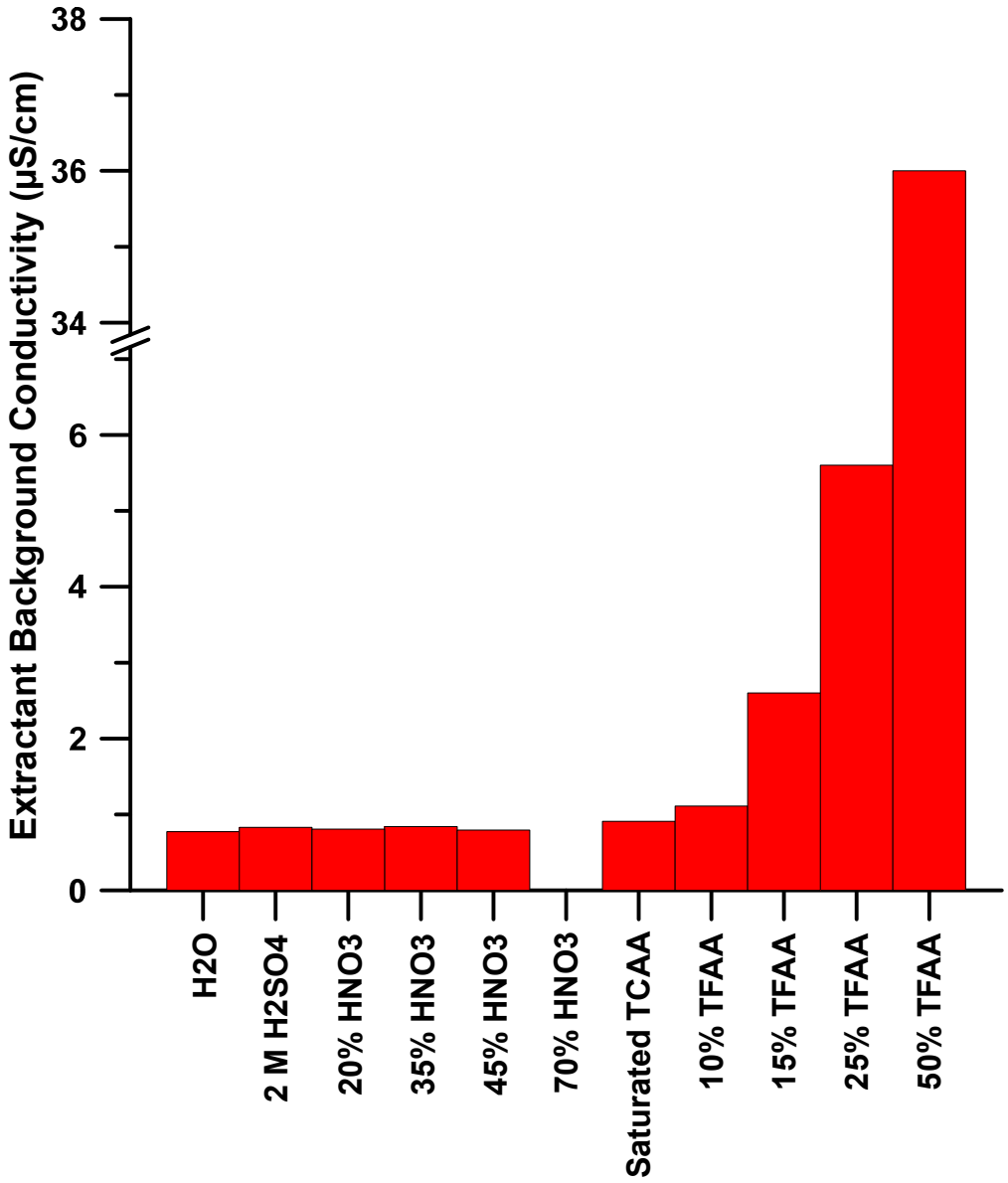

Figure S11. The extractant conductivity is plotted vs. the extractant solution used. 70% nitric acid was not allowed to interact with the membrane long enough to record a reading in the extractor due to the very high penetrant conductance observed and possible damage to the membrane. Some impurity is likely present in the trifluoroacetic acid (TFAA). Nitric acid was ICP-MS grade and showed no interference.

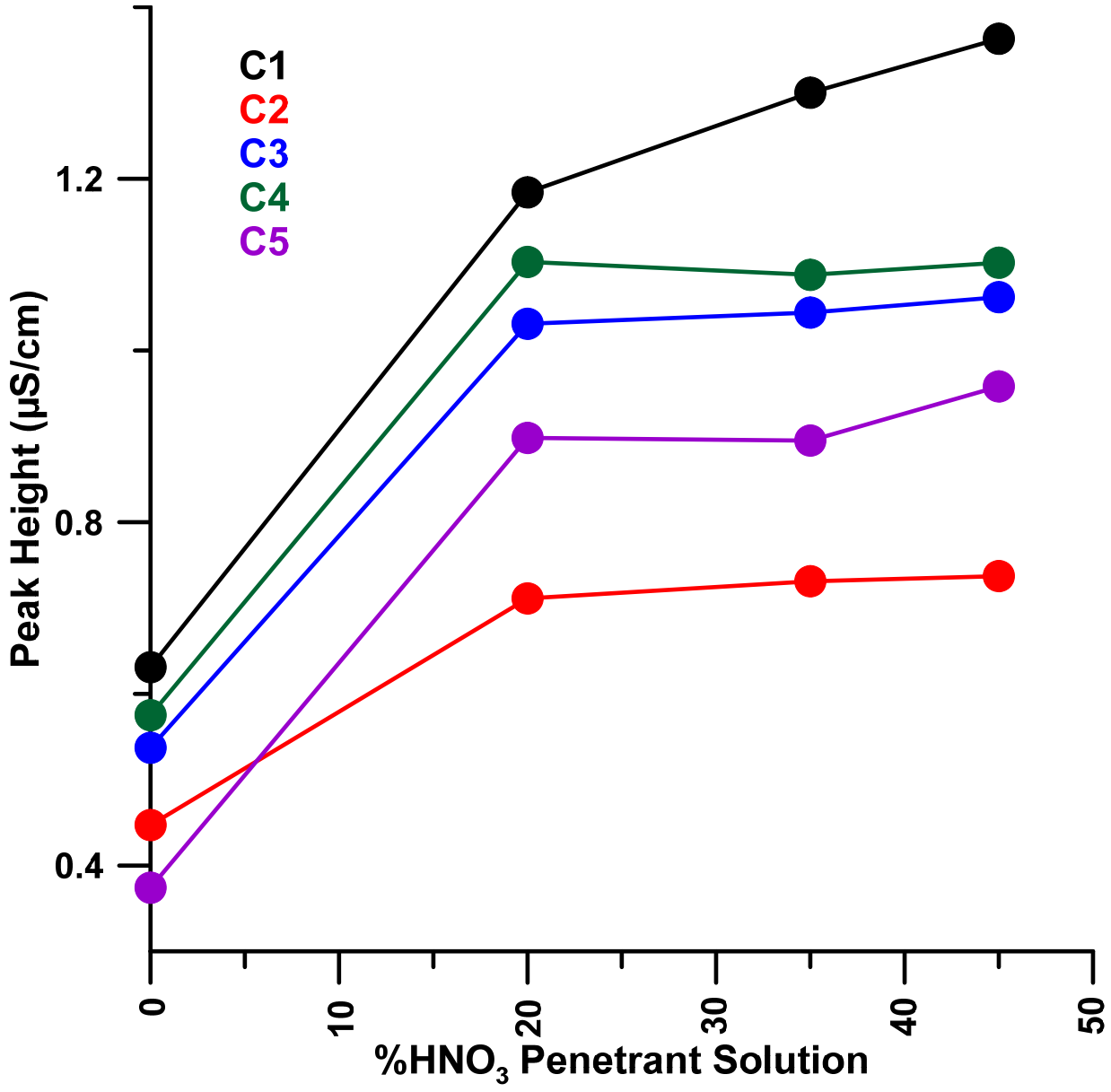

Figure S12 The concentration of HNO_3 acid penetrant is plotted against the peak height of 5 aliphatic acids. The penetrant lowers the effluent pH which increases the amount of undissociated acid that can permeate through the membrane. Formate, which has the lowest pK_a, shows the greatest increase in peak height. Other acids are less dissociated due to their higher pK_a and show no improvement above ~20% HNO_3. For formate this is effect is still quite small. The eluent concentration is 0.5 mM $HClO_4$.

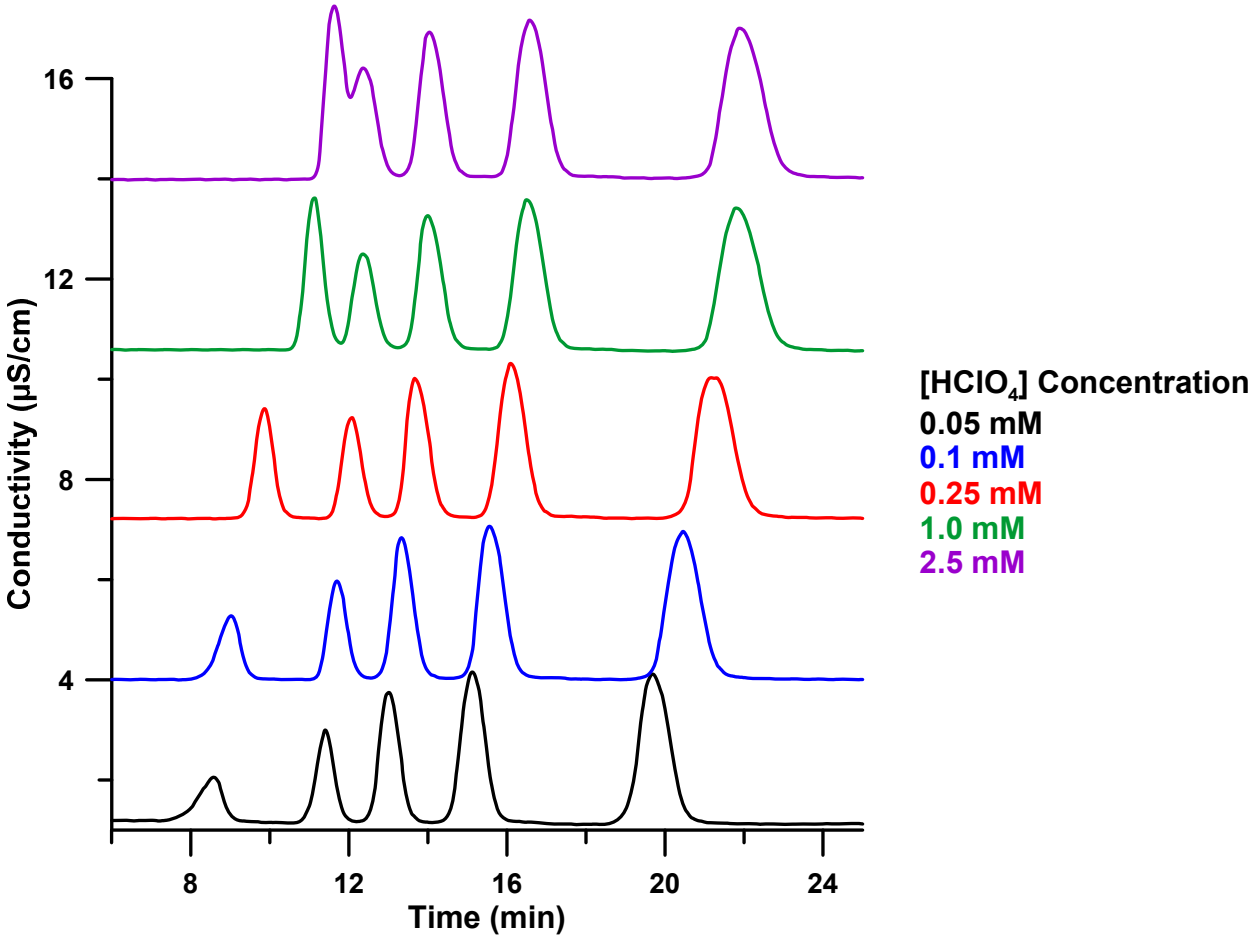

Figure S13. The retention dependence of C1-C5 VFAs on the eluent acid concentration. Retention increases with increasing $HClO_4$ eluent concentration. This effect reaches a maximum when acid dissociation is entirely suppressed and no change in retention occurs with a further increase in eluent acid concentration. No penetrant was used in these experiments. The peak heights can be seen visually decreasing with decreasing eluent concentration, particularly for formate. At low eluent concentrations (<0.25 mM) the formate peak begins to front. Other conditions as in Figure S3.

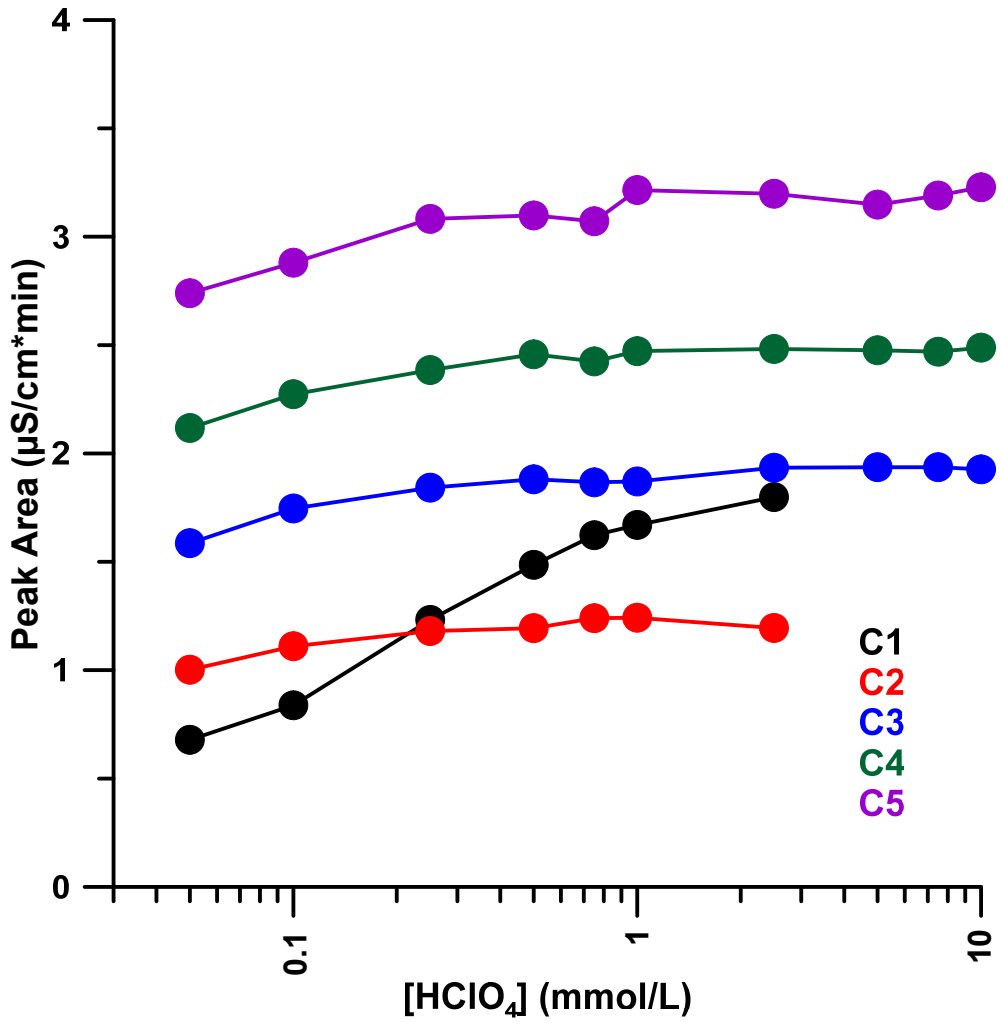

Figure S14. The peak area of the peaks from Figure S13 are plotted against the eluent $HClO_4$ concentration. At low $HClO_4$ concentrations the peak area of all the weak acids begins to decrease because of greater dissociation and less unionized acid to permeate through the membrane. A plateau is reached at higher eluent acid concentrations where the analyte is almost entirely unionized. The relatively high analyte concentrations used here likely represent a best case scenario for transfer especially at the lowest $HClO_4$ concentrations where the weak acid is contributing more to lowering the pH than the eluent.

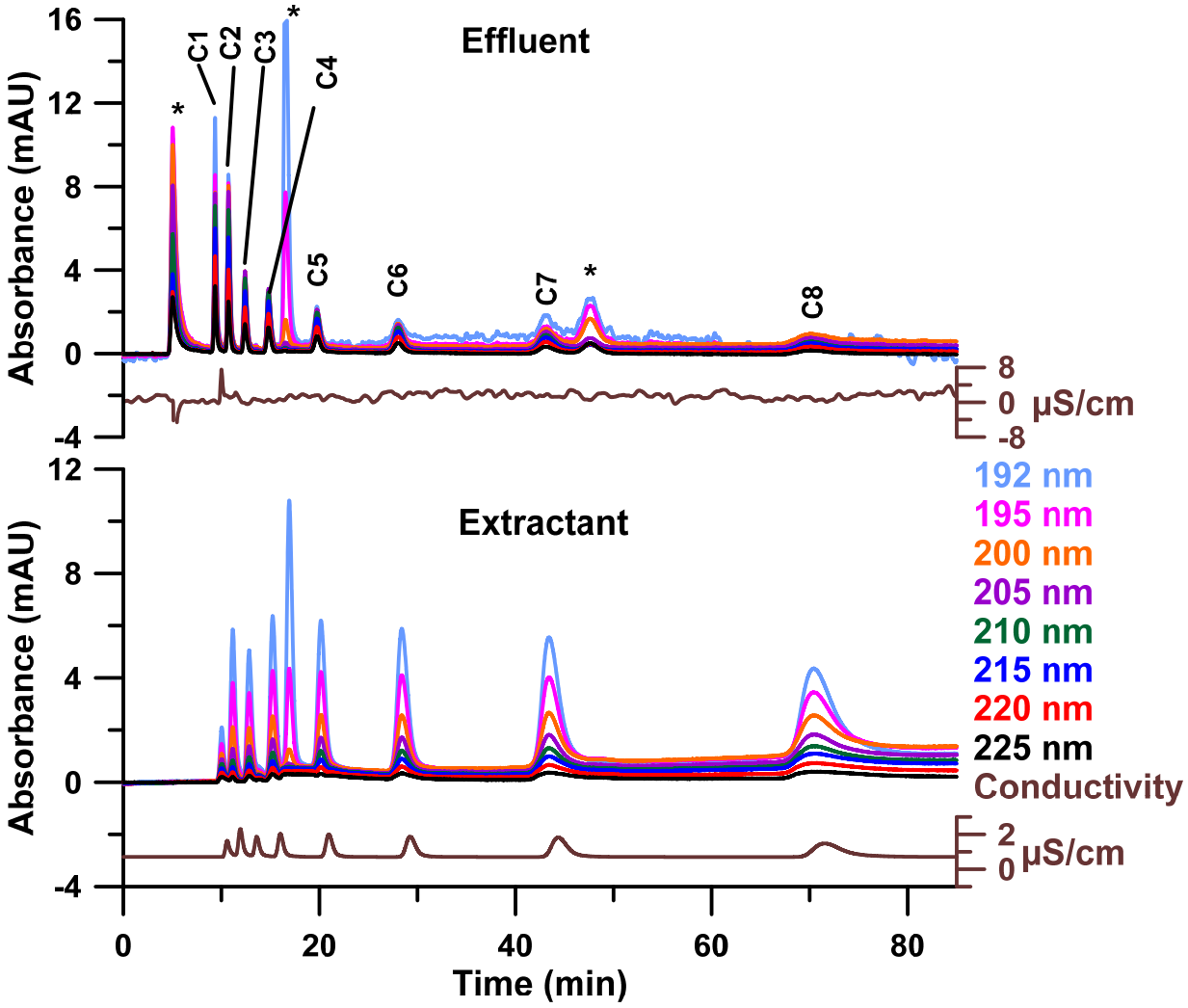

Figure S15. UV-Vis absorbance (8 different wavelengths) and conductance chromatograms of 8 VFAs measured both in the extractant and effluent. 1 mM $HClO_4$ eluent. 10 µL injection. VFA concentrations are as follows (C1-C8, respectively): 150, 300, 200, 200, 250, 300 mg/L, 350, and 400 mg/L. The considerably higher concentrations injected reflect the relative insensitivity of UV detection compared to conductivity. EFR 0.1 mL/min. Only the C1 peak can be observed in the effluent conductivity trace. Unknown peaks are marked with an asterisk. The peak eluting after C4 is likely CO_2. The peak eluting after C7 is clearly an impurity and clearly also less volatile than the other acids. The absorbance ratios in the extractant and effluent are not the same because of greater ionization in the extractant and greater absorption by the carboxylate. No penetrant was used.

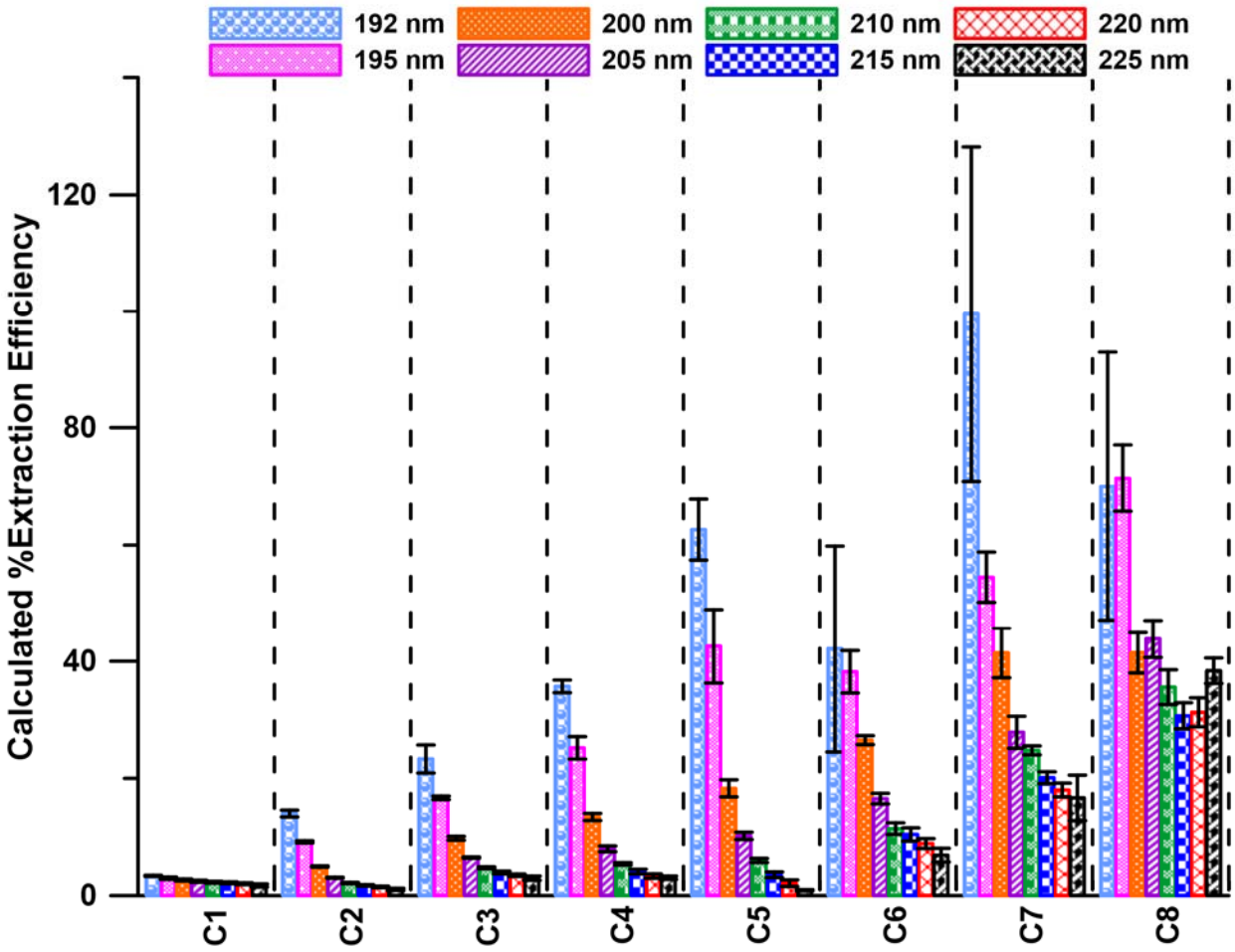

Figure S16. Calculated extraction efficiencies based on absorbance peak areas. The different flow rates in the lumen and the jacket were taken into account. For all but C1, the FAVE extractant absorbance detection is more sensitive than measuring absorbance directly in the column effluent due to the large difference in absorption for the carboxylate and carboxylic acid. The FAVE also is less prone to interferences and has a lower background noise and fewer interfering peaks.

Water Extractant Peak Areas and Extraction Efficiency Calculation.

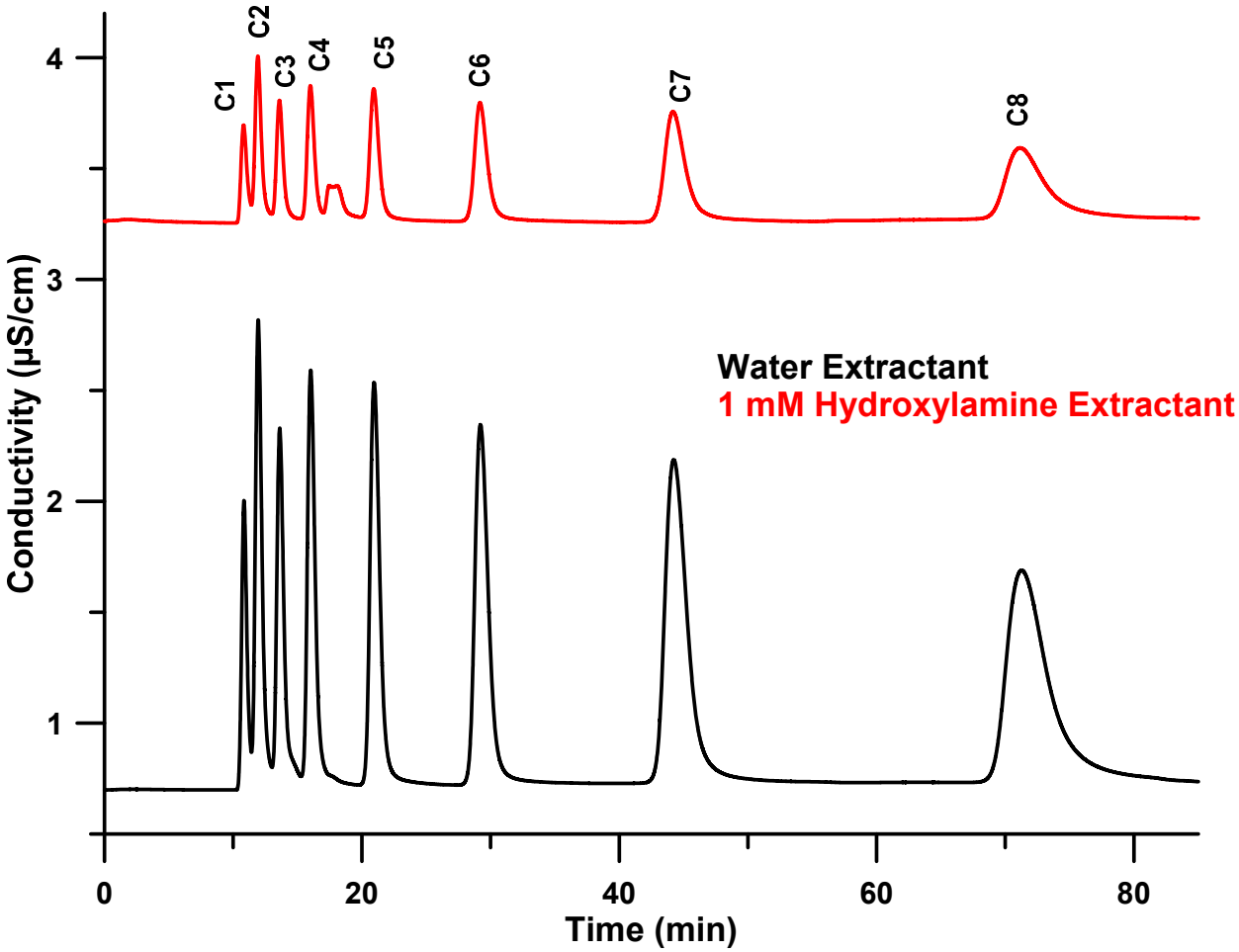

Figure S17. Bottom: FAVE water extract signals elicited by 10 µL injections of C1-C8 VFAs, concentrations listed in Table S2. Top: Same experiment with 1 mM hydroxylamine (HA) as extractant. Notice the additional peak, presumably due to a much weaker acid (and thus not directly visible with a water extractant), between C4 and C5 that is visible with HA as the extractant.

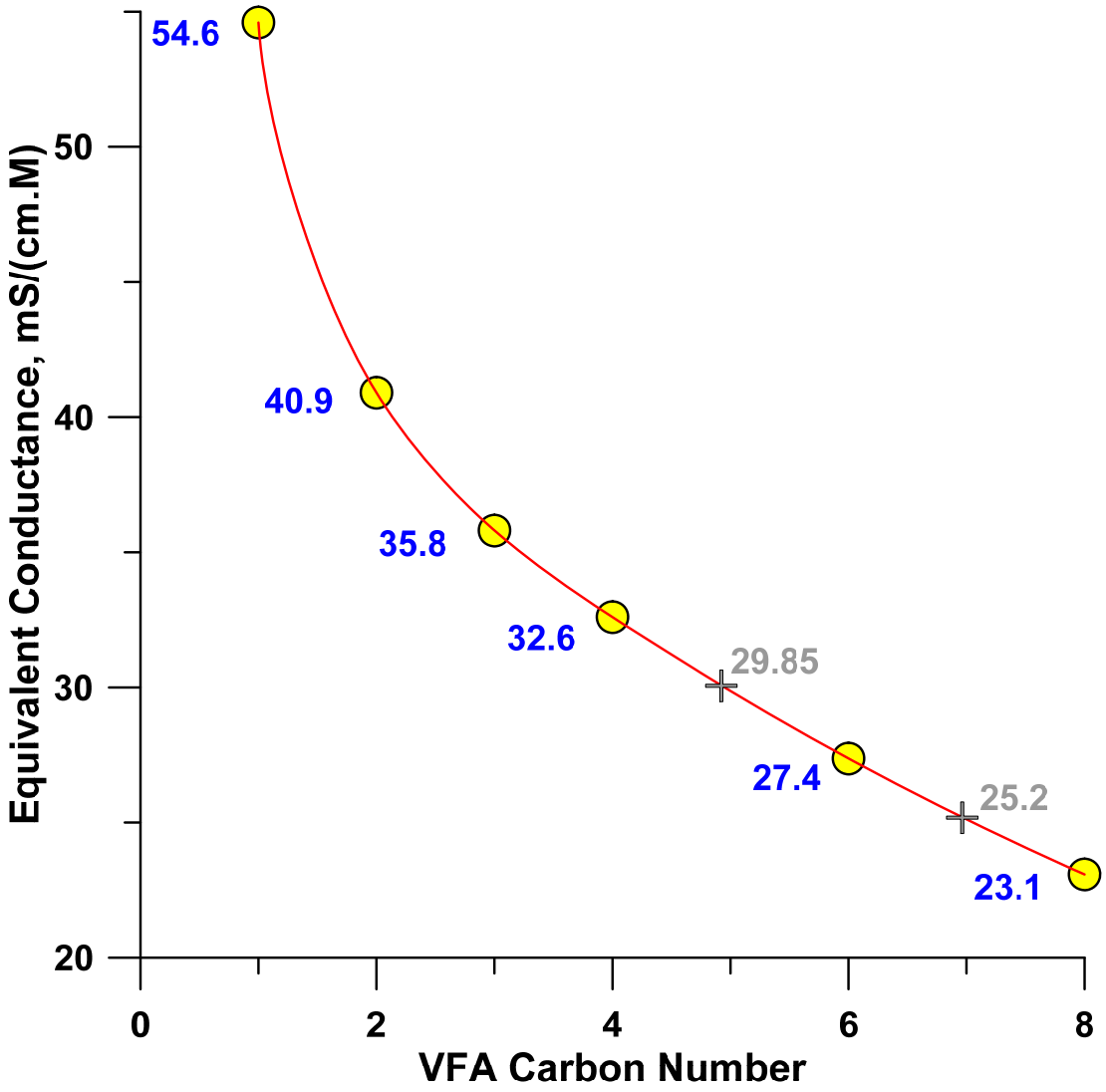

Figure S18. Equivalent conductance values for C1-C8 VFA anions. The values in blue are from the literature the other two are interpolated from the spline fit.

The equivalent conductance of all the VFA anions are needed for this calculation. Those for C1-C4 acids are found commonly[5] and those for the C6 and the C8 acid has been reported in the literature:[6,7] those for C5 and C7 were determined by interpolation as shown above in Figure S18.

Table S1. Estimation of Ionization in the FAVE extract and FAVE Extraction Efficiency (EE)[a]

Name	pKa	Ka	Peak ht FAVE Water extract µS/cm (sd) n=3	VFA anion equivalent conductance, mS/(cm.M)	Ionized VFA equivalent conductance, mS/(cm.M)	Ionized VFA Concn at peak, M	Unionized VFA, M [Ionized VFA]^2/Ka	Total VFA, M	Percent Ionization at Peak	Percent Ionization at half peak concentration
Formic	3.75	1.78E-04	1.37 (0.02)	54.6	404.4	3.39E-06	6.45E-08	3.45E-06	98.1	99.0
Acetic	4.76	1.74E-05	2.17 (0.01)	40.9	390.7	5.55E-06	1.77E-06	7.33E-06	75.8	84.8
Propionic	4.87	1.35E-05	1.63 (0.02)	35.8	385.6	4.23E-06	1.32E-06	5.55E-06	76.1	85.1
Butyric	4.82	1.51E-05	1.88 (0.02)	32.6	382.4	4.92E-06	1.60E-06	6.51E-06	75.5	84.6
Valeric	4.84	1.45E-05	1.82 (0.02)	29.85	379.7	4.79E-06	1.59E-06	6.38E-06	75.1	84.3
Hexanoic	4.88	1.32E-05	1.64 (0.02)	27.37	377.2	4.35E-06	1.43E-06	5.78E-06	75.2	84.4
Heptanoic	4.89	1.29E-05	1.45 (0.02)	25.2	375.0	3.87E-06	1.16E-06	5.03E-06	76.9	85.7
Octanoic	4.90	1.26E-05	0.90 (0.02)	23.08	372.9	2.41E-06	4.63E-07	2.88E-06	83.9	90.6
				Injected	**Peak Area**	**% Ionization**	**nmol**			
	mg/L	**MW**	**mM**	**nmol**	**µS.mL/cm**	**Corrected**	**in FAVE**	**Percent**		
						Peak Area	**Extract**	**EE**		
Formic	150	46.025	3.26	32.6	0.067	0.068	0.167	**0.51**		
Acetic	300	60.05	5.00	50.0	0.133	0.157	0.401	**0.80**		
Propionic	200	74.08	2.70	27.0	0.112	0.132	0.341	**1.26**		
Butyric	200	88.11	2.27	22.7	0.141	0.167	0.436	**1.92**		
Valeric	250	102.13	2.45	24.5	0.175	0.208	0.547	**2.23**		
Hexanoic	300	116.16	2.58	25.8	0.218	0.258	0.685	**2.65**		
Heptanoic	350	130.18	2.69	26.9	0.303	0.354	0.943	**3.51**		
Octanoic	400	144.2	2.77	27.7	0.344	0.380	1.02	**3.67**		

[a]The top half of this table estimates the extent of ionization at each peak apex by dividing the peak height by the equivalent conductance of the fully ionized VFA. Given the ionized concentration (C_I), the unionized concentration C_u is computed as C_I^2/K_a; the fractional ionization is then computed as 100* C_i/ (C_i + C_u). If the average concentration in the peak is taken as half the peak concentration, the degree of ionization at this average concentration appears in the last column.

In the bottom half, the observed peak area is corrected using the average degree of ionization in the last column at the top and then converted to moles using the equivalent conductance data for the fully ionized VFA. Extraction efficiency is then computed as the fraction of the amount injected.

Table S2. FAVE Extraction Efficiency with 1 mM Hydroxylamine as FAVE Extractant

VFA	1 mM Hydroxylamine FAVE Extractant Peak Area (n=3) nS.mL/cm	Hydroxylammonium Salt of VFA, equivalent Conductance mS/(cm.M)	Computed HA Salt in Extract nmol	Extraction Efficiency % EE	Average % EE
Formic	24.3 (0.1)	122.6	0.198	**0.61**	**0.56**
Acetic	45.3 (0.3)	108.9	0.416	**0.83**	**0.82**
Propionic	36.3 (0.6)	103.8	0.350	**1.30**	**1.28**
Butyric	42.6 (0.5)	100.6	0.423	**1.87**	**1.89**
Valeric	56.0 (1.1)	97.85	0.572	**2.34**	**2.29**
Hexanoic	66.3 (0.7)	95.37	0.695	**2.69**	**2.67**
Heptanoic	99.3 (2.0)	93.2	1.065	**3.96**	**3.73**
Octanoic	121.6 (1.4)	91.08	1.34	**4.81**	**4.24**

The data in blue is the extraction efficiency computed from the peak area and the equivalent conductance of a fully ionized hydroxylammonium-VFA salt. The last column depicts the averages of the EE computed here and that in Table S1.

We also performed a separation using pure water as an eluent so that conductivity detection could be used in the main column effluent as well. This results in shorter retention and poorer resolution amongst the acids as well as peak fronting. Compared to the sample used in the experiments in Table S1 and S2, the sample was diluted 320x. C7 and C8 acids were sufficiently well separated from others and based on a comparison of the main column effluent vs. the FAVE extractant signals, the respective %EE values were computed to be 3.5 ± 0.2, and 4.1 ± 0.3, in excellent agreement with the averaged EE for these two VFAs in Table S2.

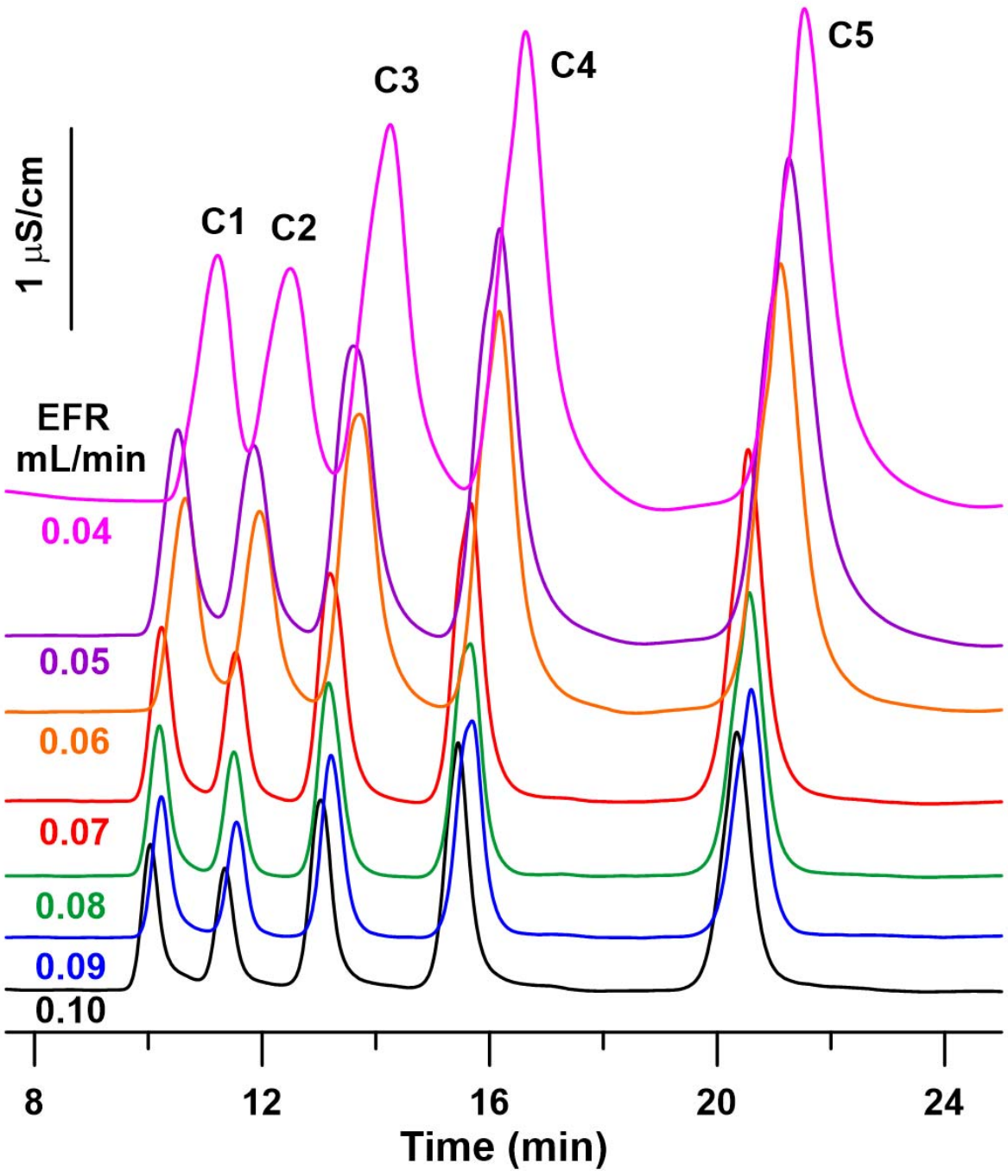

Figure S19. Chromatograms produced using different extraction flow rates for FAVE 6. The efficiency increases with increasing flow rate till the linear velocity in both the extraction portion and effluent portions are the same. The higher flow rate results in dilution of the analyte and lower sensitivity. Concentrations: C1,C2: 60 mg/L, C3,C4: 80 mg/L, C5: 100 mg/L, 20 μL injected. Pneumatic delivery was used to deliver fluid at 0.04 mL/min. No penetrant was used, eluent contains 1 mM $HClO_4$. Higher flow rates could not be used due to the backpressure of the device

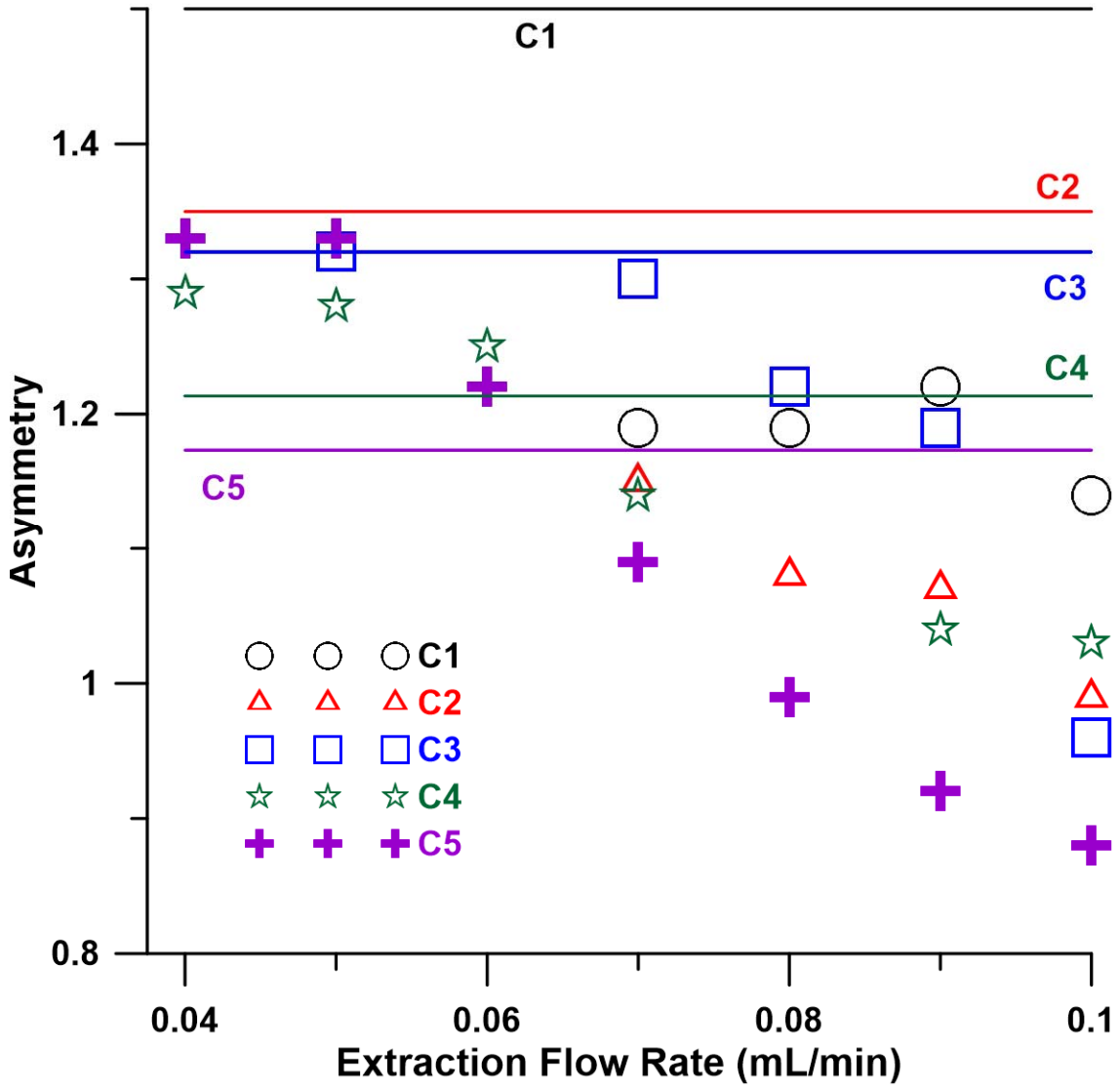

Figure S20. Solid lines show peak asymmetries (all measured at 5% peak height) for the analyte peaks exiting the FAVE lumen as seen by UV absorbance at 210 nm; this is essentially independent of the EFR. This should be considered the input function when considering the asymmetry of the FAVE extract peaks. C1 and C2 peak asymmetries at low EFR showed high variance and are not shown. C1 enters with the narrowest peak and highest asymmetry and the extractant peak asymmetry changes relatively the most, becoming more symmetric, i.e. the transfer process involves fronting but asymmetry does not further change much in the EFR range studied. At the lowest EFR studied the C3 peak asymmetry is the same as the input asymmetry suggesting this may be close to the isokinetic region. C4 and C5 have greater asymmetry than the input at the lowest two flow rates but does not change between these flow rates again suggesting this may be close to the isokinetic region. For all the other data, asymmetry continuously decreases, For all analytes except C1, at EFR ≥ 0.06 mL/min, the asymmetry decreases monotonically, the transfer involves peak fronting that increases with increasing EFR, consistent with higher flow velocities increasingly higher than isokinetic. Sample and separation conditions are identical to those in Figure S19.

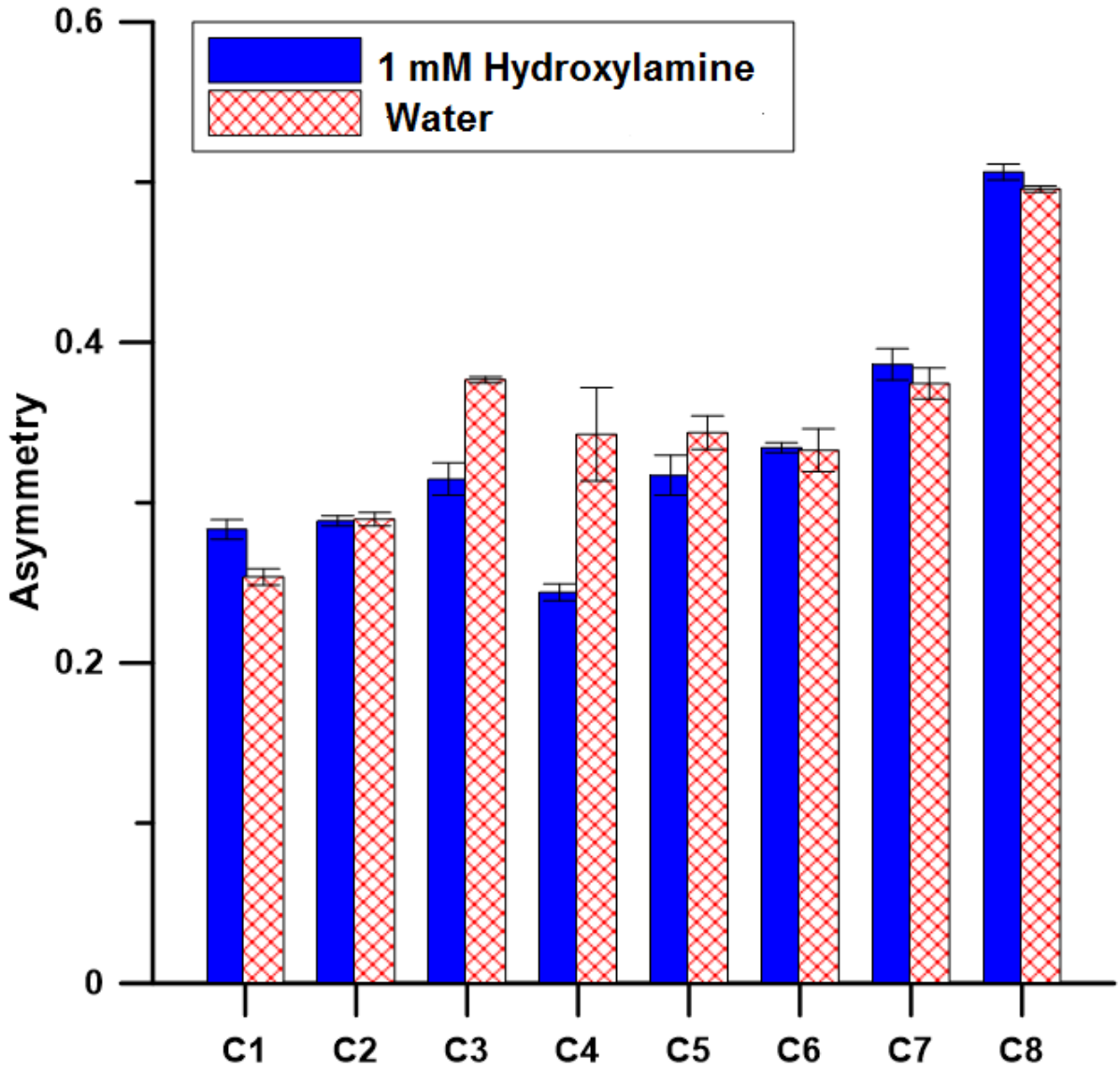

Figure S21. Asymmetry of C1-C8 VFA peaks water vs. 1 mM hydroxylamine extractant. FAVE 6. 1 mM $HClO_4$ eluent, no penetrant, FAVE 6, EFR 0.1 mL/min. Sample, 10 μL, VFA concentrations are as follows (C1-C8, respectively): 150, 300, 200, 200, 250, 300 mg/L, 350, and 400 mg/L. Other conditions as in Fig. S15.

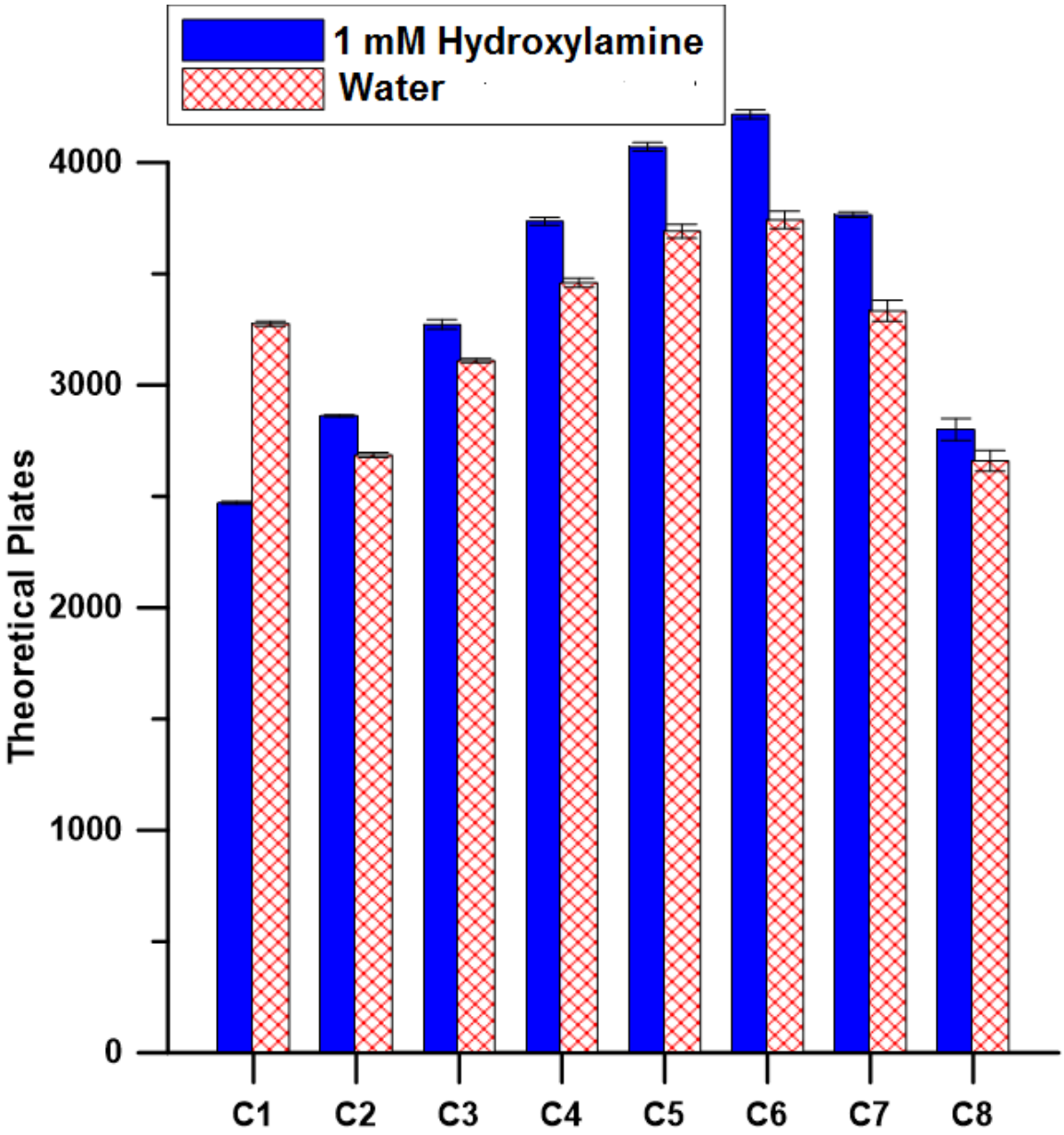

Figure S22. Observed efficiencies, water vs. hydroxylamine extractant in FAVE 6. Other conditions as in Fig. S15.

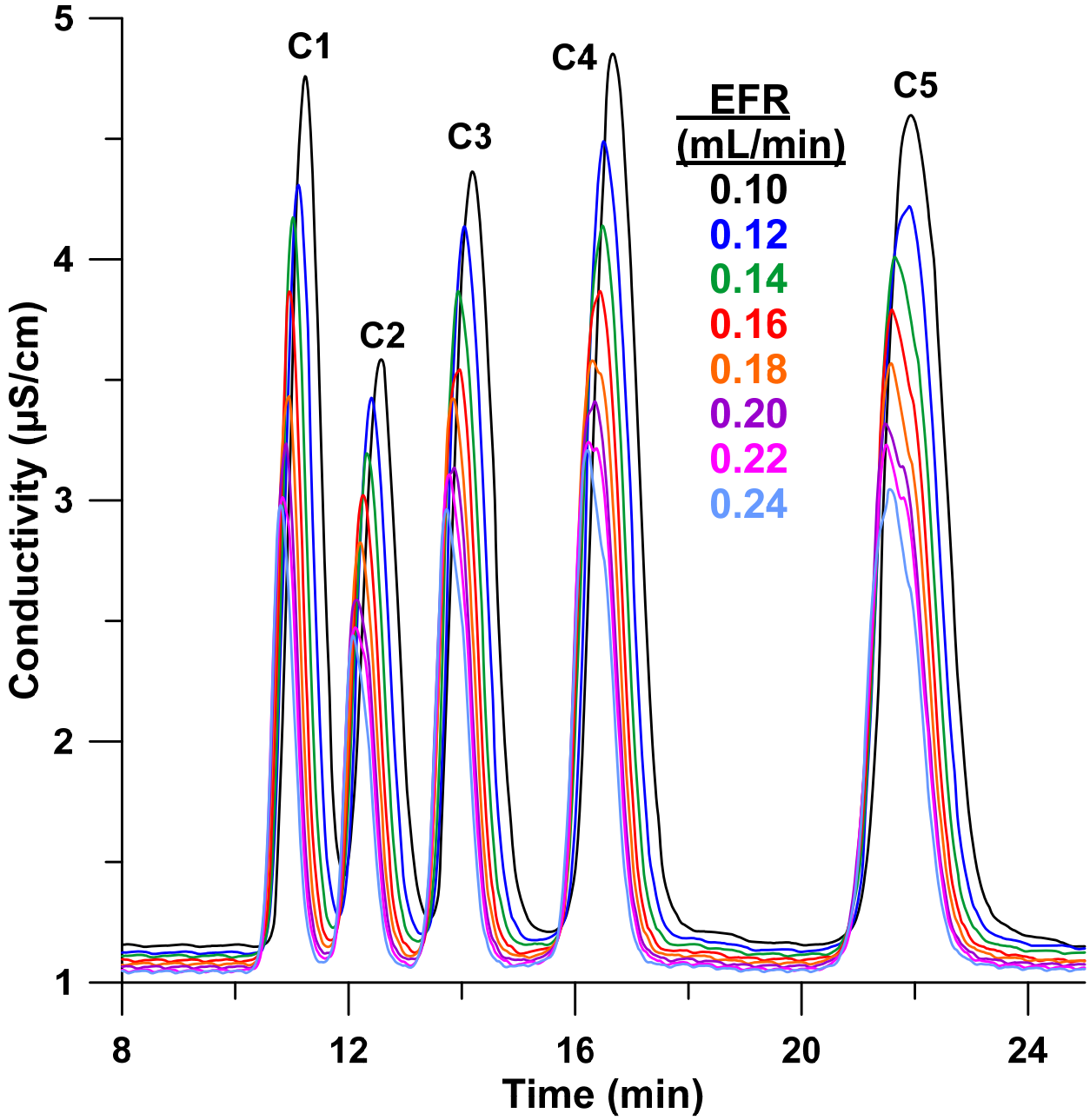

Figure S23. Chromatograms produced using different extraction flow rates for FAVE 3: the filament filled siloxane VPMT extractor. The higher flow rate results in dilution of the analyte and lower sensitivity. No penetrant was used, eluent was 1 mM $HClO_4$.

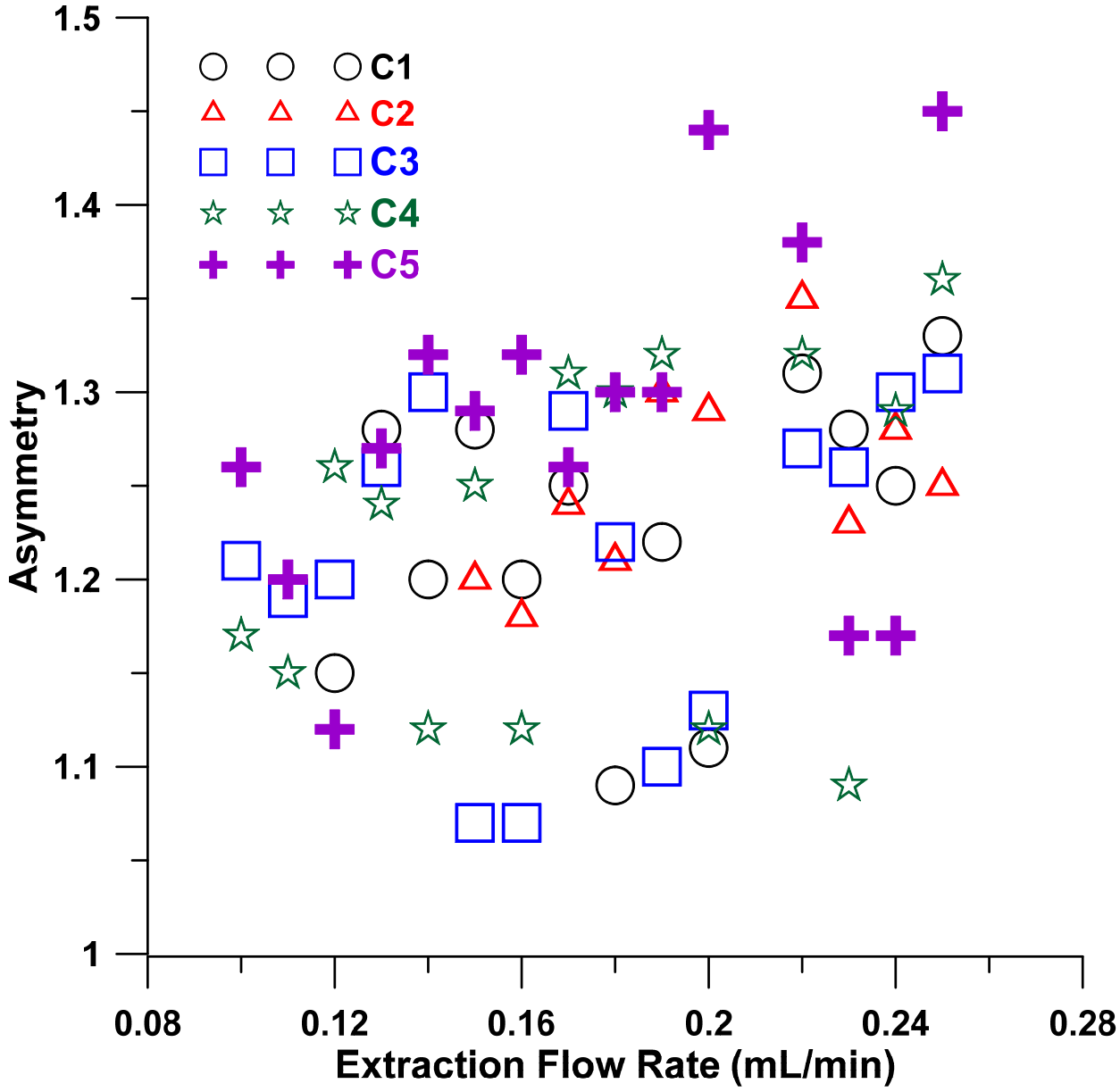

Figure S24. Asymmetry data for the experiments in Figure S23. FAVE 3.

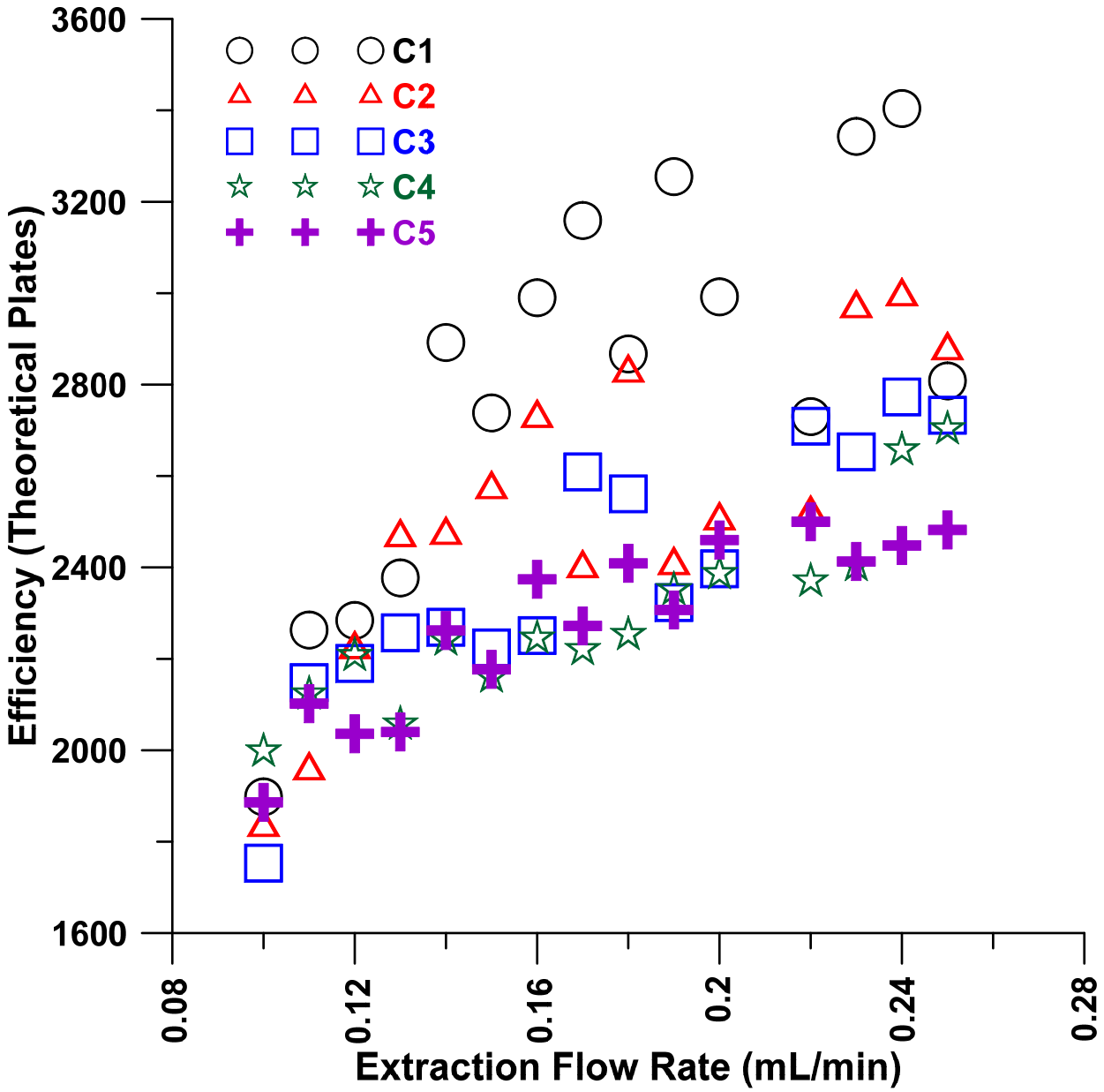

Figure S25. Efficiency data for the experiments in Figure S23. FAVE 3.

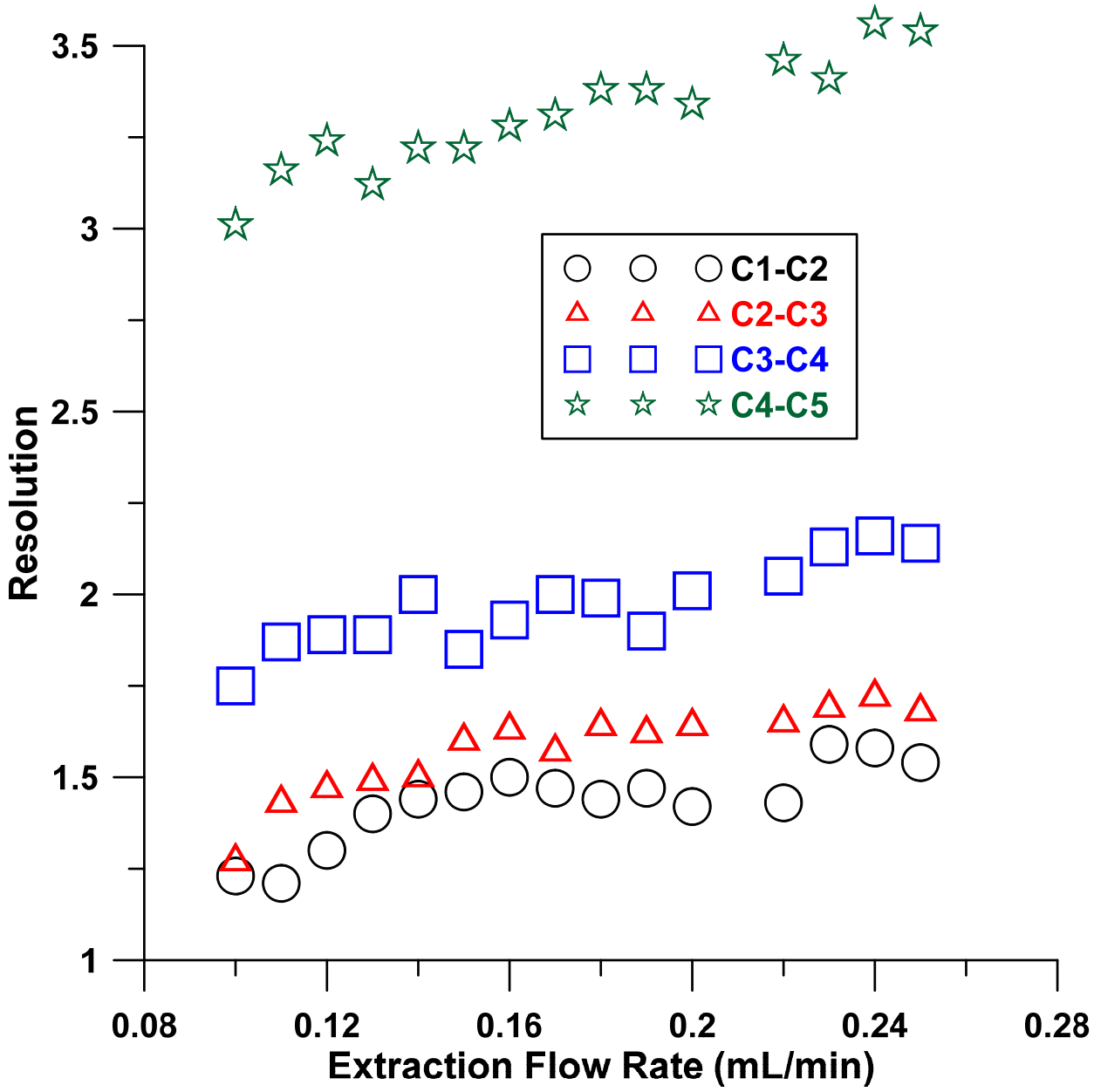

Figure S26. Resolution data for the experiments in Figure S23. FAVE 3.

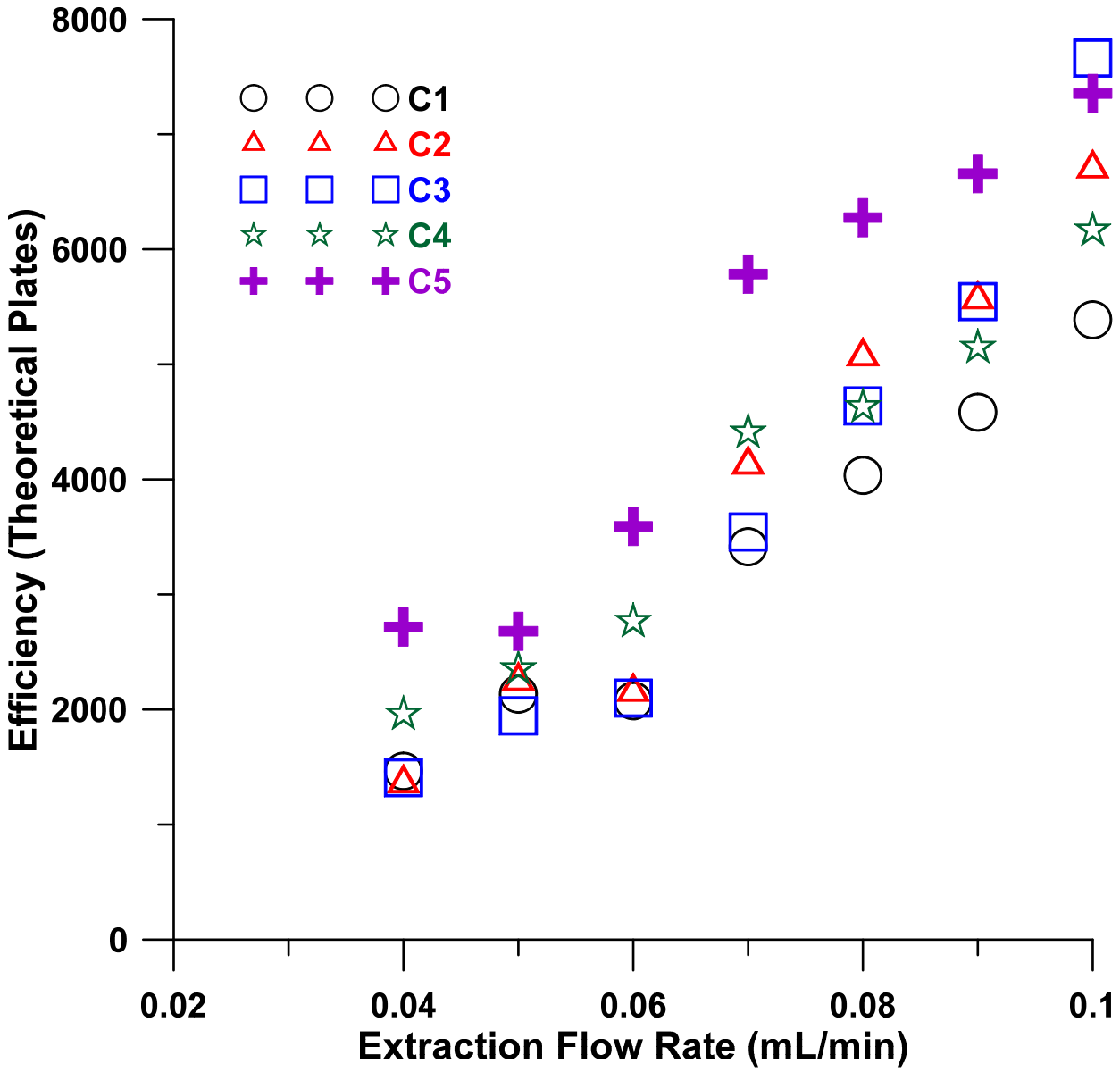

Figure S27. Efficiency data for the results in Figure S20. FAVE 6.

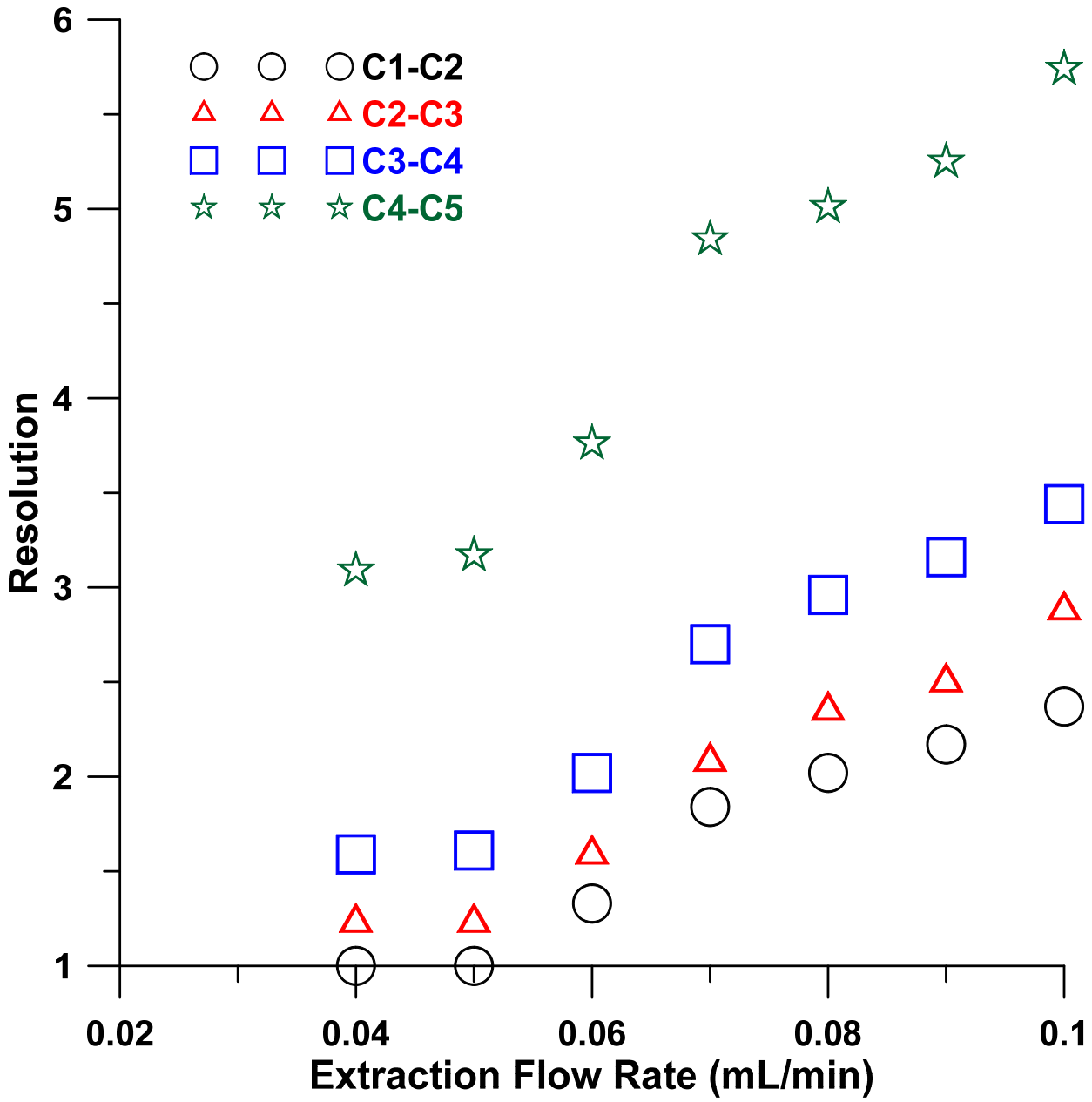

Figure S28. Resolution data for the results in Figure S20. FAVE 6.

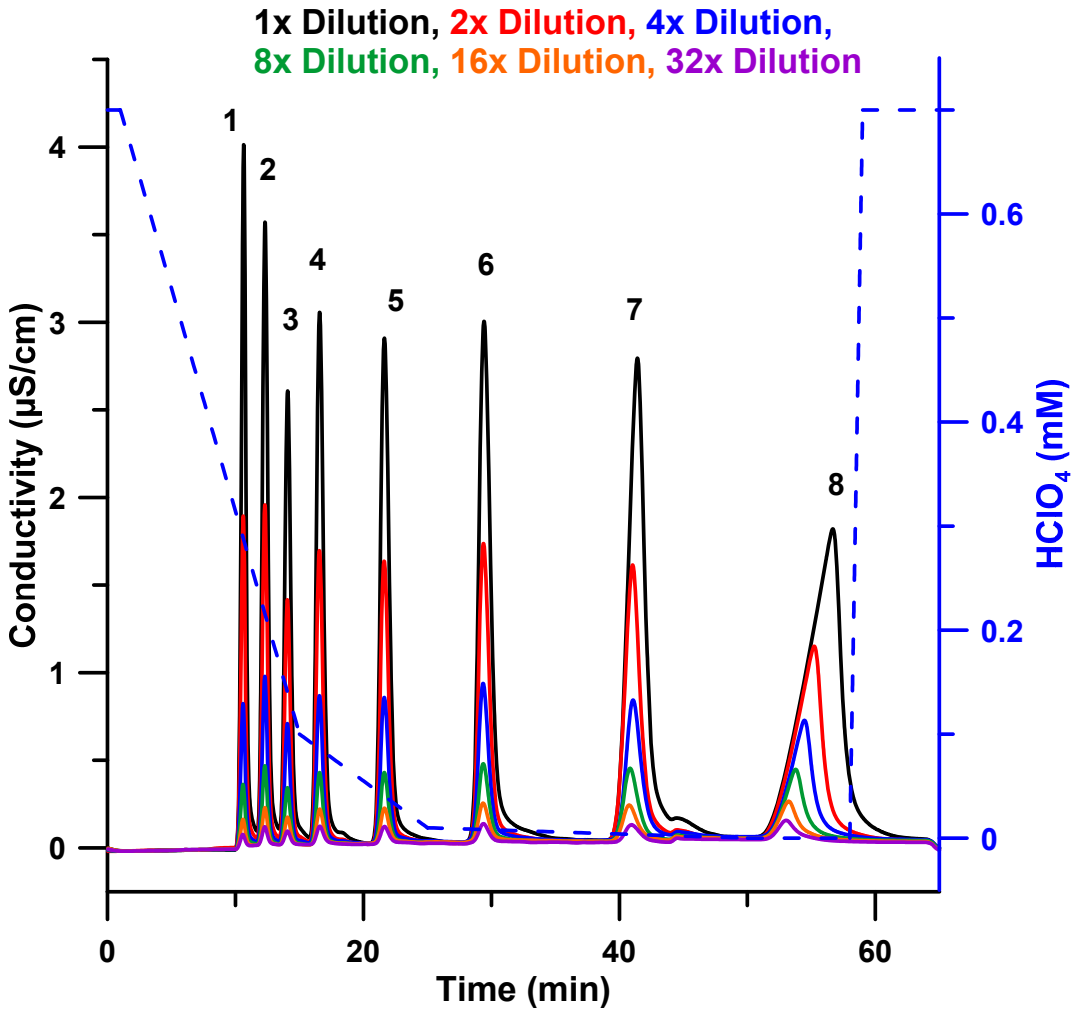

Figure S29. Gradient separation of C1-C8 VFAs. The blue dashed line is the $HClO_4$ acid gradient used. Fronting is observed for the C8 VFA due to the absence of acid during its elution. This effect is reduced at lower concentrations of standard. Penetrant is 25% HNO_3, EFR 0.075 mL/min, pneumatic pumping. VFA concentrations in the undiluted standard are as follows (C1-C8, respectively): 30, 60, 40, 40, 50, 60, 70, and 80 mg/L.

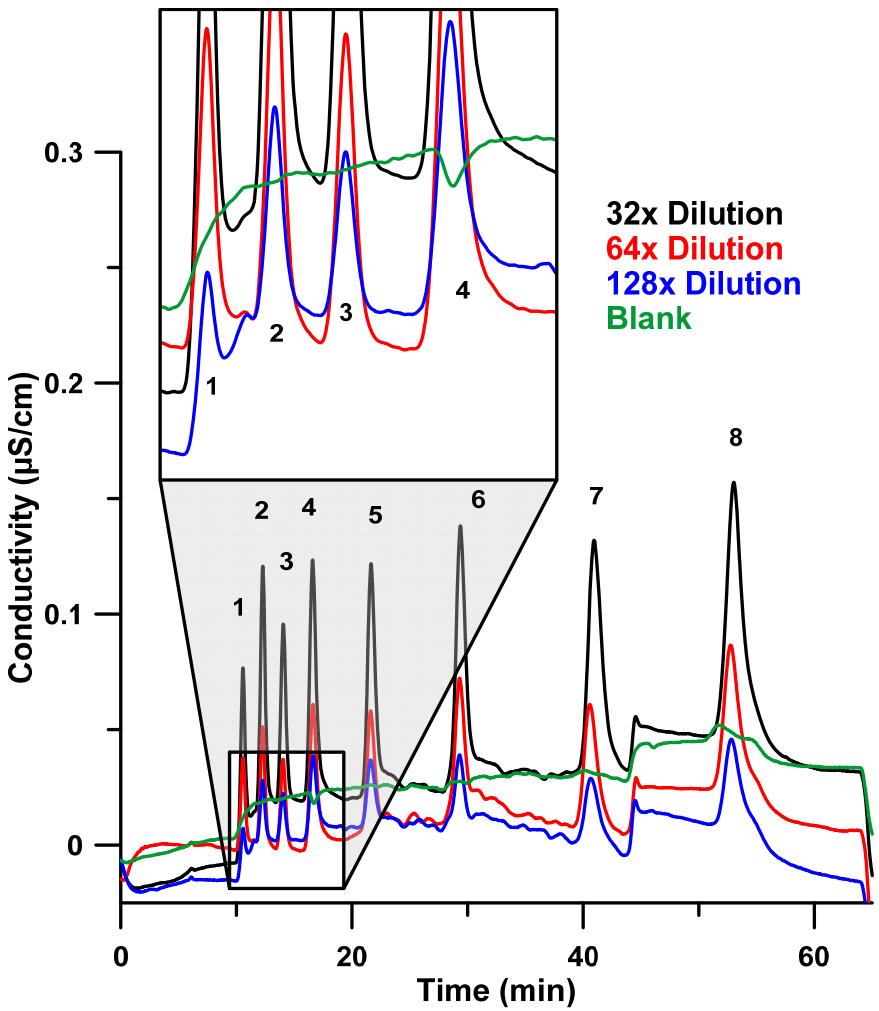

Figure S30. Gradient separation of low concentrations of C1-C8 VFAs using the gradient in Figure S29. The indicated dilution factors refer to the original sample composition in Figure S29. Background shift caused by the change in eluent composition is <50 nS. Peak to peak noise is typically between 1-3 nS.

Table S3. Retention Data as a function of concentration and Eluent[a]

	Original Sample					2x Dilution		4x Dilution	
Analyte	Concn	1 mM $HClO_4$ Eluent		Water Eluent		Water Eluent		Water Eluent	
Acid	µM	α_0	t, min[b]	α_0	t, min	α_0	t, min	α_0	t, min
Formic	40.7	0.849	5.567	0.016	0.733	0.007	0.450	0.004	0.328
Acetic	62.4	0.983	7.037	0.076	3.017	0.045	2.467	0.026	2.106
Propionic	33.7	0.987	8.817	0.050	3.917	0.032	3.350	0.019	2.978
Butyric	28.4	0.985	11.367	0.039	4.783	0.024	4.150	0.014	3.717
Valeric	30.6	0.986	16.617	0.028	6.617	0.017	5.867	0.010	5.345
Hexanoic	32.3	0.987	25.410	0.021	9.867	0.014	8.900	0.008	8.200
Heptanoic	33.6	0.987	41.423	0.017	15.667	0.011	14.483	0.007	13.484
Octanoic	34.7	0.988	70.650	0.009	25.550	0.006	23.750	0.004	22.644

[a]Assuming half of detected peak concentration or half of injected peak concentrations made no significant difference in the α_0 values. [b]The retention times with the $HClO_4$ eluent does not vary with sample concentration.

Table S4. Parameters Computed From Data in Table S3, Best Fit to Eq. 3

Carbon No	R_{an}	R_u	R_u/R_{an}	Linear r^2
1	0.45	6.48	14.46	0.9970
2	2.29	7.14	3.12	0.9855
3	3.22	8.91	2.77	0.9868
4	4.02	11.49	2.86	0.9899
5	5.74	16.78	2.93	0.9933
6	8.74	25.64	2.93	0.9949
7	14.22	41.78	2.94	0.9967
8	23.67	71.25	3.01	0.9978

The data in columns 2 and 3 come from the best fits to eq. 3 (the linear r^2 for which appears in column 5); and the ratio of these two terms appears in column 4.

Gradients with Other Additives. Admittedly, the difference in the analysis time between the isocratic and gradient elution approaches can stand improvement. Although several other approaches were attempted, none were better. Reported mobile phase additives to reduce retention include heptanol (0.05% v/v)**Error! Bookmark not defined.** or sucrose (150 mM).[8] In the present system, heptanol did reduce retention but the effect was rather small. It also reduced partition to the membrane, C6-C8 VFA responses were particularly reduced (Figure S31); larger modifier concentrations were hence not attempted. Adding sucrose to a 1 mM $HClO_4$ eluent paradoxically *increased* the retention of all VFAs and increasing concentrations had a greater effect; it also reduced the transfer of C6-C8 VFAs (Figure S32).

The most traditional gradient additive, acetonitrile (up to 15% v/v), allowed the separation of 8 VFAs in 40 min (Figure S33). However, even with LC-MS grade acetonitrile, the background increased with increasing acetonitrile. The conductance of pure acetonitrile is in the 30-90 nS/cm range.[9] There are two possibilities: (a) acetonitrile hydrolyzes to acetamide and then to acetic acid; this reaction has been studied at high pressures water in near critical temperatures (275-350 °C, 300 bar).[10] While the Arrhenius plot has reasonable linear correlation coefficient (r^2 0.98), extrapolating to 60 °C (the highest temperature we used) may be a stretch. But if we are to take that leap, the half-life at 60 °C will be in excess of 26,500 years; this process would not seem to be a contributor. However, this process can be catalyzed, for example by some metal complexes; [11] it is not known if the strongly acidic cation exchange resin bed can accelerate this hydrolysis. (b) The second possibility is that traces of the hydrolysis product, acetic acid is already present in the acetonitrile.

According to specifications, the titratable acid is <0.001 meq/g (1meq/L). In other words the acid content could be as high as 1 mM. 15% ACN can be equivalent to 150 µM acid However, we have previously observed that relative to pure water being pumped through an ICE column at 35-40 °C, adding 5% ACN raises the background by 2-3 µS/cm. Addition of 15% ACN thus may contribute up to 10 µS/cm. This contribution was due to some acidic impurity as adding small amounts of base reduced the background.[12] Some fraction of this will penetrate across the VPM. It is likely therefore that both processes contribute.

In any case, acetonitrile probes the occluded volume, requiring considerable re-equilibration time after the gradient is done and it also reduces VFA partition to the membrane, decreasing the sensitivity.

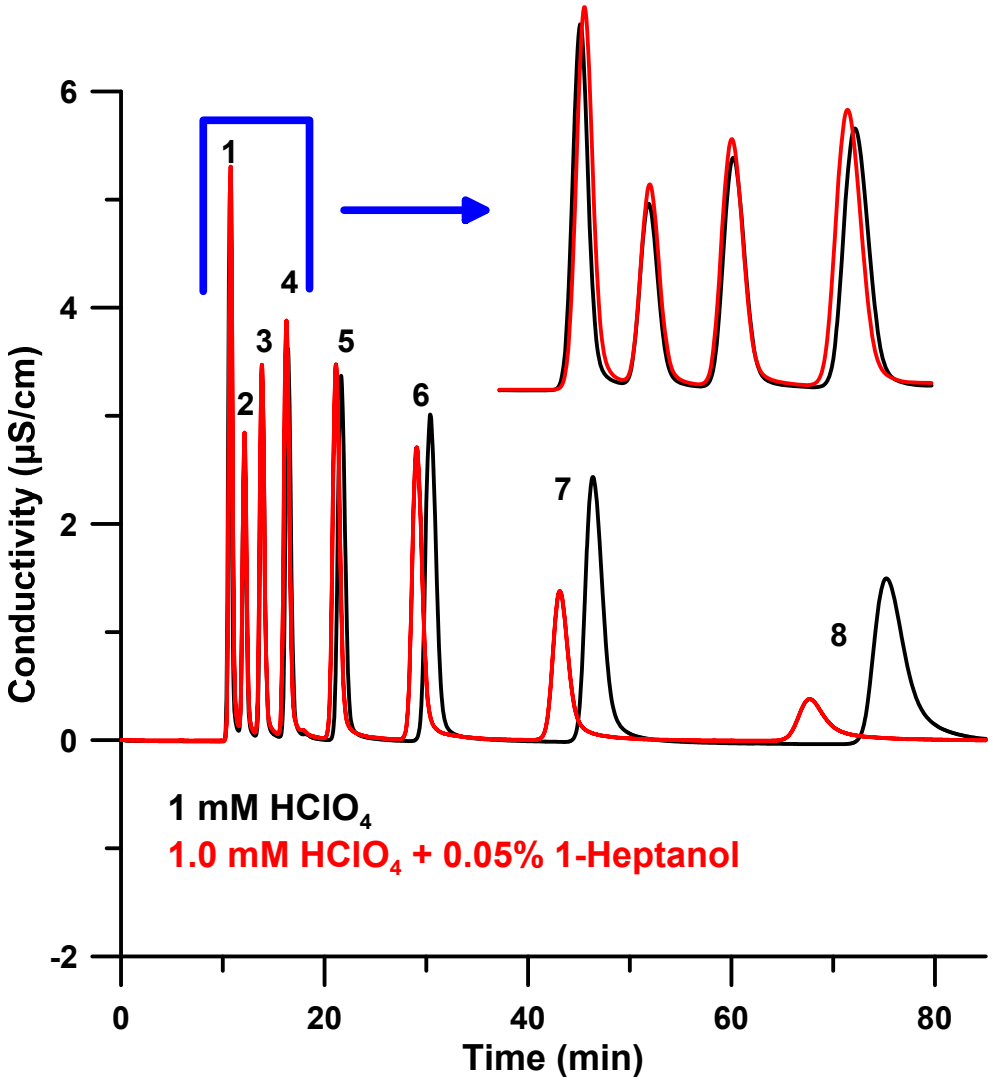

Figure S31. Isocratic elution of C1-C8 VFAs using small amounts of heptanol in the eluent. The heptanol increases partitioning of the strongly retained acids into the mobile phase some, but significantly reduce the transfer through the membrane. 20 µL injection, C1-C8: 30, 60, 40, 40, 50, 60, 70, 100 mg/L. Penetrant: 25% HNO_3. EFR 0.075 mL/min, pneumatic pumping.

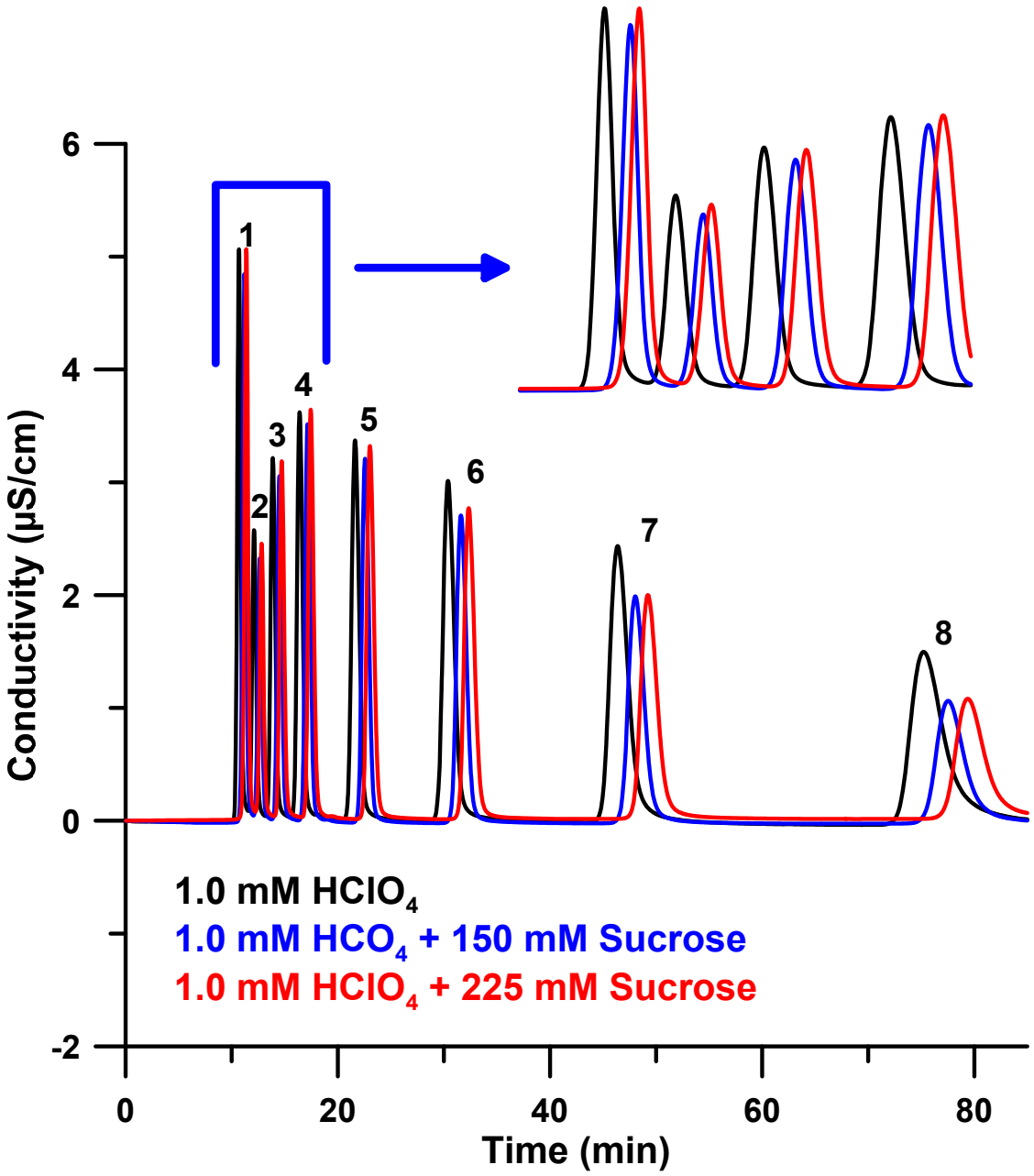

Figure S32. Isocratic elution of 8 organic acids using sucrose in the eluent. The sucrose causes all the acids to be retained longer. Some decrease in transfer efficiency is observed upon addition of sucrose to the mobile phase. Other conditions in Figure S32.

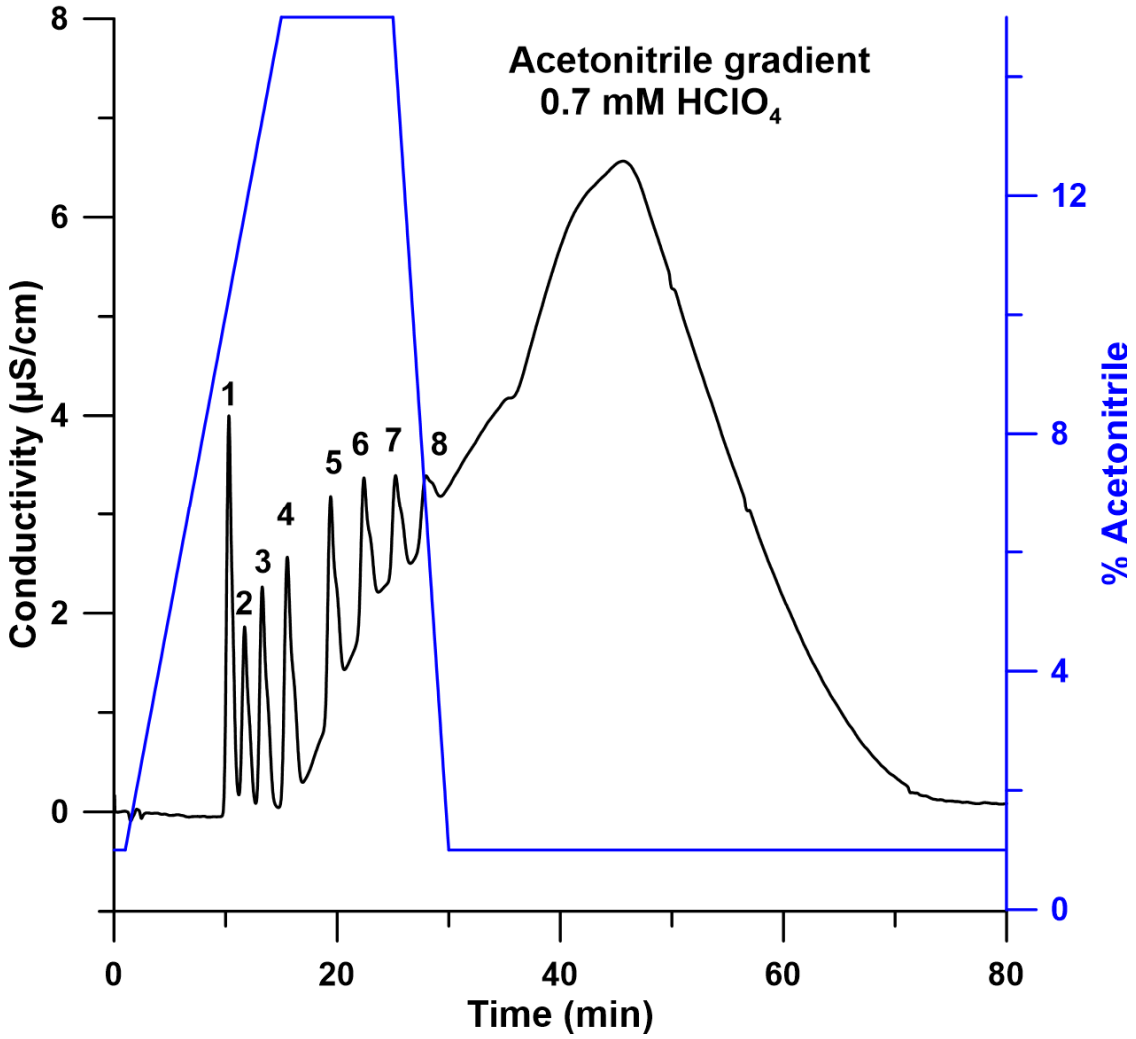

Figure S33. A gradient using acetonitrile for the separation of the C1-C8 VFAs. The acetonitrile probes the full occluded volume and though the gradient is started immediately, it takes ~13 minutes to be detected by conductivity. The acetonitrile has much greater impact on the separation than acid alone, but it lowers the vapor pressure of the acids and therefore their extraction efficiency. The acetonitrile used was LC-MS grade but still appeared to contain conductive impurities that interfere with the measurement. The impurities are retained more than the acetonitrile is as evidenced by the continual rise in baseline conductance despite the maximum acetonitrile concentration being reached and the long equilibration back to baseline. The standard contained the following acids: C1-C8: 30, 60, 40, 40, 50, 60, 70, 80 mg/L. Other conditions as in Figure S32. Extractant was pneumatically pumped at 0.075 mL/min.

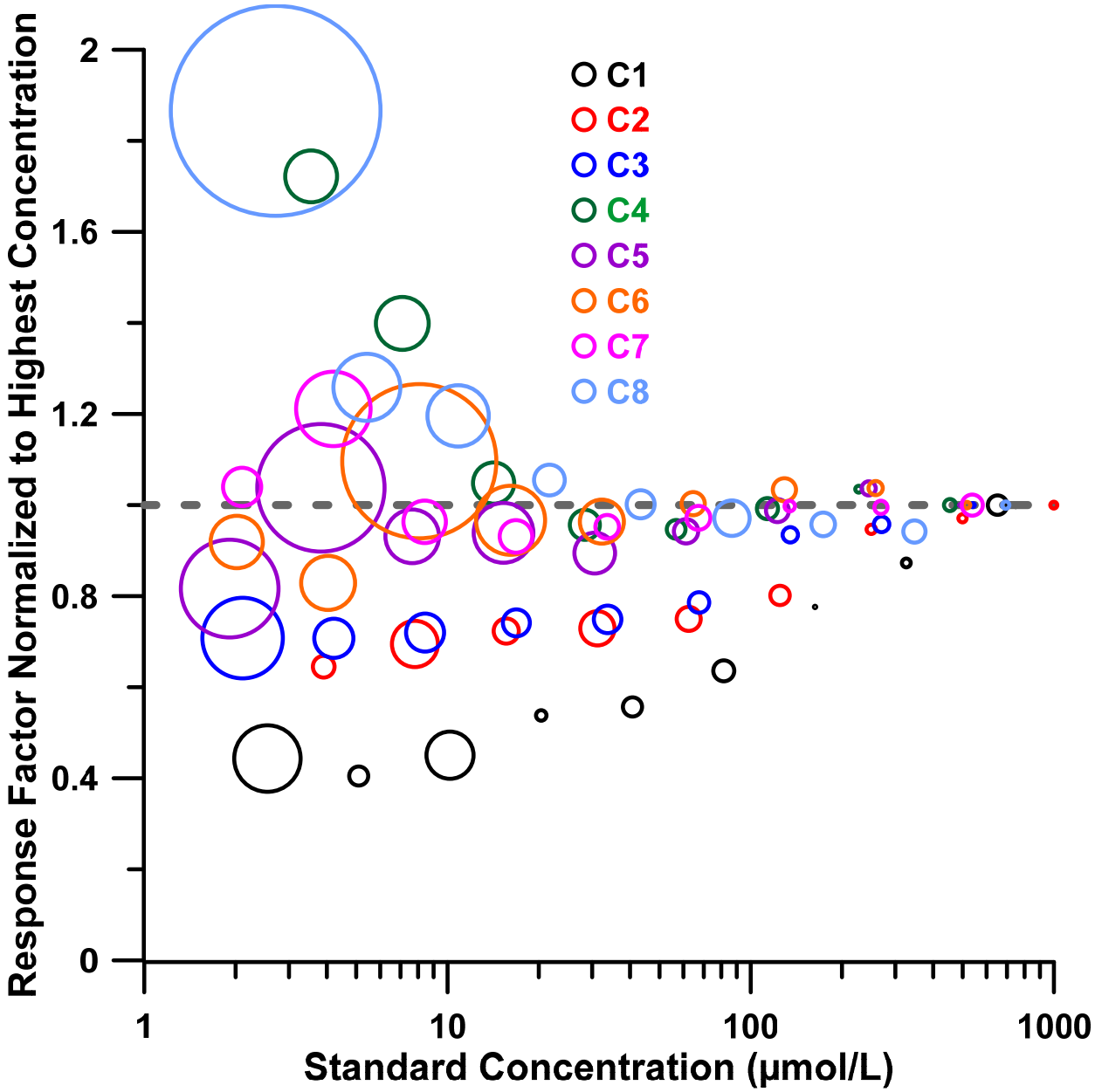

Figure S34. The response factor plot of triplicate measurements of C1-C8 VFAs. The diameter of the bubble represents two standard deviations. C1-C3 VFAs show some supralinearity while the C8 VFA shows some sublinear behavior. The cause of supralinearity is not known but carryover may lead to biases for the C8 VFA. The C4 VFA is biased by the presence of CO_2 in all samples. 25% HNO_3 is used as the penetrant. 0.075 mL/min EFR, pneumatic pumping.

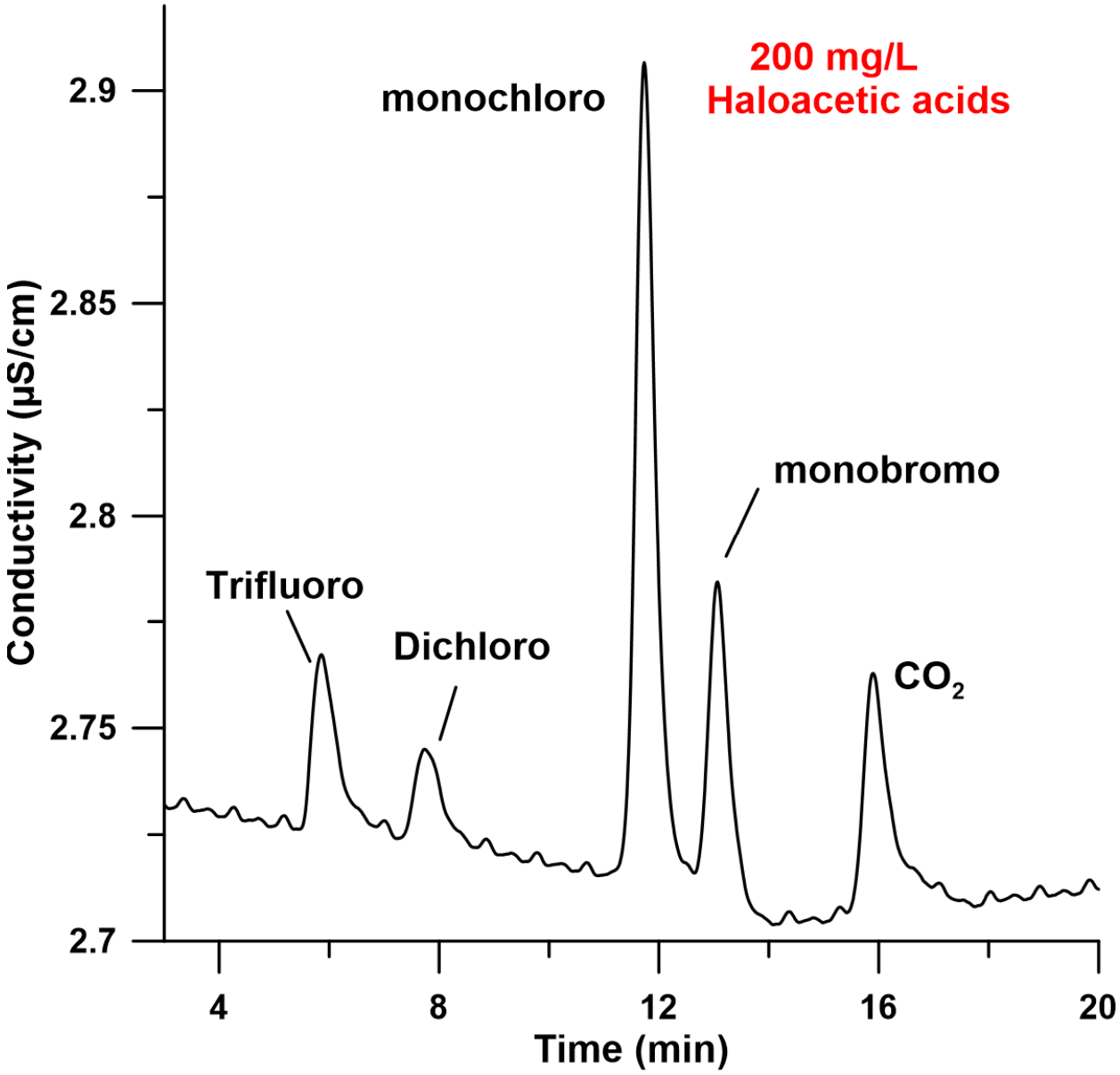

Figure S35. Haloacetic Acids extracted on Nafion Coated porous polypropylene membrane. Trichloroacetic acid likely elutes with TFA but was unable to be seen. TCA couldn't be seen at all; the lower selectivity for the membrane may be one reason it produces lower backgrounds than TFA when used as a penetrant. Acids could not be detected on a siloxane coated VPM. pKa of chloro, bromo, dichloro, trichloro and trifluoro acetic acids are, respectively: 2.86, 2.86, 1.35, 0.66, and 0.23. Eluent was 10 mM $HClO_4$.

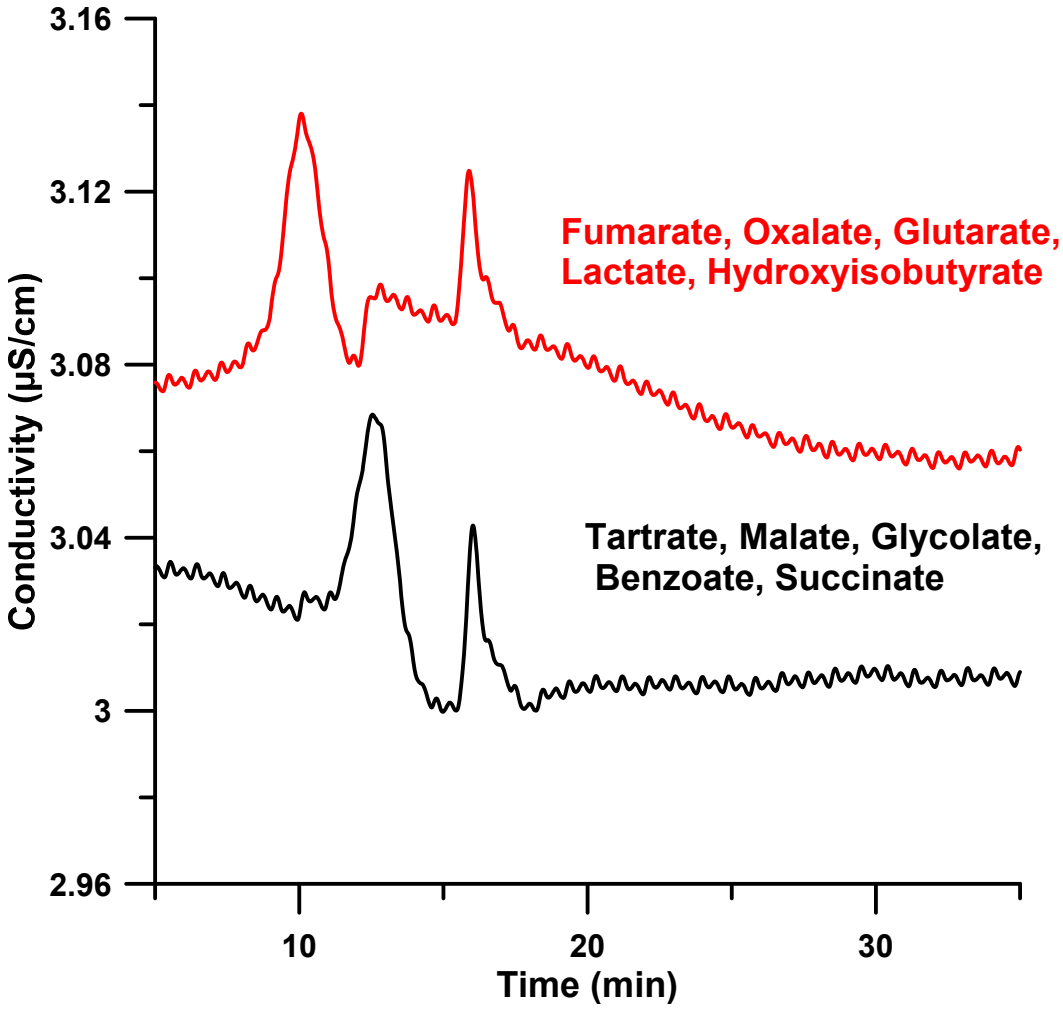

Figure S36. Extraction of various nonvolatile weak acids. All concentrations were 50 mg/L. CO_2 can be seen at ~16 min. It is not clear what is eluting before this, but it is not any of the acids added to the mix. FAVE 6, 25% HNO_3 penetrant, EFR 0.1 mL/min

Table S5. Analytical Data for Real Samples

				Solution Concentration (mg/L)													
	Mass/ volume?	Sample Mass (g) / initial volume (mL)	Final Volume (mL)	Formic		Acetic		Propionic		Butanoic		Hexanoic		Heptanoic		Octanoic	
				Average	Stdev	Average	Stdev	Average	Stdev	Average	Stdev	Average	Stdev	Average	Stdev	Average	Stdev
Yogurt Sample 1	mass	0.29	10.00	35.4	0.60	73.7	2.14	ND	ND	3.94	0.33	9.14	2.87	ND	ND	14.0	7.23
Yogurt Sample 2	mass	0.24	10.00	32.5	0.17	98.2	1.10	ND	ND	5.88	0.82	10.9	0.65	ND	ND	13.4	0.53
Yogurt Sample 3	mass	0.37	10.00	20.0	0.49	59.0	0.20	ND	ND	3.82	0.57	7.21	0.41	ND	ND	6.96	1.19
SauerKraut Brine	volume	1.00	25.00	6.16	0.30	2440	21.8	ND	ND	8.88	0.33	ND	ND	ND	ND	ND	ND
Pickle Brine	volume	1.00	25.00	4.14	0.66	8440	99.6	ND	ND	12.1	3.02	ND	ND	ND	ND	ND	ND
Pickle Brine	volume	1.00	250.00	13.7	2.44	7750	25.9	ND	ND	79.5	4.30	ND	ND	ND	ND	ND	ND
Balsamic Vinegar	volume	1.00	25.00	244	34.1	44100	31.4	ND	ND	3.88	0.64	ND	ND	ND	ND	ND	ND
Balsamic Vinegar	volume	1.00	1000.00	180	7.33	51700	935	ND	ND	295	255	ND	ND	ND	ND	ND	ND
Yogurt Sample 1-2	mass	1.03	25.00	585	61.0	275	11.0	ND	ND	297	12.5	8.70	1.82	ND	ND	15.7	3.23
Yogurt Sample 2-2	mass	1.01	25.00	778	55.1	389	16.9	ND	ND	345	13.5	12.6	1.59	ND	ND	14.2	ND
Yogurt Sample 3-2	mass	1.03	25.00	300	24.1	115	8.73	ND	ND	245	5.47	6.06	0.67	ND	ND	14.4	ND
Yogurt Sample 4-2	mass	1.01	25.00	215	11.5	84.1	0.50	ND	ND	274	4.46	4.76	0.62	ND	ND	10.6	3.28
Tofu	mass	0.99	25.00	2.25	0.75	33.9	0.35	ND	ND	38.1	1.25	ND	ND	ND	ND	ND	ND
Yogurt 1000 mM HClO4	mass	5.07	10.00	9.02	0.10	31.5	0.69	0.02	0.01	1.56	0.05	2.04	0.15	?	?	ND	ND
Yogurt 500 mM HClO4	mass	4.89	10.00	7.98	0.07	27.9	0.11	0.02	0.01	1.61	0.06	1.96	0.07	?	?	ND	ND
Yogurt 100 mM HClO4	mass	4.73	10.00	7.79	0.08	23.1	0.23	0.03	0.00	1.57	0.06	1.84	0.04	?	?	1.55	0.04
Yogurt 1000 mM HClO4	mass	5.07	25.00	8.88	0.28	29.6	0.49	ND	ND	1.69	0.19	1.91	0.06	ND	ND	1.56	0.54
Yogurt 500 mM HClO4	mass	4.89	25.00	7.98	0.33	26.8	0.72	ND	ND	1.52	0.13	1.87	0.18	ND	ND	1.56	0.14
Yogurt 100 mM HClO4	mass	4.73	25.00	7.62	0.05	21.9	0.19	ND	ND	1.40	0.17	1.85	0.13	ND	ND	1.30	0.33

REFERENCES

(1) Liao, H.; Kadjo, A. F.; Dasgupta, P. K. *Analytical Chemistry* **2015**, *87*. 8342-8346.
(2) Liu, Y.; Srinivasan, K. Pohl, C.; Avdalovic, N. *J. Biochem. Biophys. Meth.* **2004,** *60*, 205-232.
(3) Dasgupta, P. K. *Analytical Chemistry* **1984**, *56*. 96-103.
(4) Blandamer, M. J.; Burgess, J. Duce, P. P. Robertson, R. E.; Scott, J. W. M. *Can. J. Chem.* **1981,** *59,* 2845-2847.
(5) Christian, G. D. Dasgupta, P. K.; Schug, K. *Analytical Chemistry* , 7th ed. Wiley, New York, 2013. P678
(6) Friesen, J. I. *Can. J. Chem.* **1960,** 38, 1939-1945
(7) Campbell, A. N.; Kartzmark, E. M.; Lakshminarayanan, G. R. *Can. J. Chem.* **1960,** 40, 839-844.
(8) Tanaka, K.; Ohta, K.; Fritz, J. S.; Lee, Y. S.; Shim, S. B. *J. Chomatogr. A* **1995**, *706*, 385-393.
(9) Cunningham, G. P.; Vidulich, G. A.; Kay, R. L. *J. Chem. Eng. Data,* **1967,** *12,* 336–337.
(10) Venardou, E.; Garcia-Verdugoa, E.; Barlowa, S. J.; Gorbaty, Y. E.; Poliakof, M. *Vib. Spectrosc.* **2004,** *35,* 103–109
(11) Concolino, T. E.; Eglina, J. L.; Staples, R. J. *Polyhedron,* **1999,** *18,* 915-921.
(12) Liao, H.; Shelor, C. P.; Dasgupta, P. K. *Anal. Chem.* **2016**, 88, 4965-4970.